Electronic Transactions on Numerical Analysis.
Volume 55, pp. 744–791, 2022.
Copyright © 2022, Kent State University.
ISSN 1068–9613.
DOI: 10.1553/etna_vol55s744

ETNA
Kent State University and
Johann Radon Institute (RICAM)

SYNCHRONOUS AND ASYNCHRONOUS OPTIMIZED SCHWARZ METHODS FOR POISSON'S EQUATION IN RECTANGULAR DOMAINS*

JOSÉ C. GARAY†, FRÉDÉRIC MAGOULÈS‡, AND DANIEL B. SZYLD§

Dedicated to Olof B. Widlund on the occasion of his eightieth birthday.

Abstract. Convergence results for optimized Schwarz methods (OSM) applied as solvers for Poisson's equation in a bounded rectangular domain with Dirichlet (physical) boundary conditions and zeroth-order (Robin) artificial transmission conditions between subdomains are presented. The analysis presented applies to a continuous formulation on an arbitrary number of subdomains with cross points. Both synchronous and asynchronous versions of OSM are discussed. Convergence theorems are presented, and it is shown numerically that the hypotheses of these theorems are satisfied for certain configurations of the subdomains. Additional numerical experiments illustrate the practical behavior of the methods discussed.

Key words. asynchronous iterations, optimized Schwarz methods, infinite-dimensional operator

AMS subject classifications. 65F10, 65N22, 65N55

1. Introduction. Our overarching goal is to solve very large linear systems arising from the discretization of PDEs using parallel iterative methods in extreme-scale supercomputers. Synchronous iterative algorithms are parallel iterative algorithms in which iterations and communications are synchronized among processors. In this synchronous paradigm, any load imbalance or nonuniformity in hardware performance causes processing units to idle at the synchronization point, waiting for the slowest unit, and thus affecting the overall performance. Thus, given the heterogeneous and distributed architecture of exascale computers, idle times in processing units will be an issue in terms of efficiency.

State-of-the-art solvers based on appropriately preconditioned Krylov subspace methods can be very fast (in terms of iteration count), but they are inherently synchronous methods. Consequently, when these methods are used as solvers in exascale computers with hundreds of thousands of processors, the communication among processors is expected to be the bottleneck, implying low efficiency and long execution times.

Asynchronous iterative algorithms are parallel iterative algorithms in which communications and iterations are not synchronized among processors. Thus, as soon as a processing unit finishes its own calculations, it can start the next cycle with the latest data received during a previous cycle, without waiting for any other processing units to finish their assigned work. These algorithms increase the number of updates in some processors (with respect to the synchronous case) but suppress idle times. This usually results in a reduction of the (execution) time to achieve convergence. For surveys of asynchronous iterations, see [3, 19, 37]. See also the historical references cited in Section 5.

Classical Schwarz methods are Domain Decomposition (DD) methods in which the transmission conditions between subdomains are Dirichlet boundary conditions [11, 39]. Optimized Schwarz methods are DD methods in which the transmission conditions contain an operator of the form $\frac{\partial}{\partial \nu} + \Lambda$, where ν is the normal derivative pointing outwards and Λ is an

*Received October 17, 2017. Accepted July 11, 2022. Published online on September 16, 2022. Recommended by Lothar Reichel. Supported in part by the U.S. Deparment of Energy under grant DE-SC0016578.

†Center for Computation & Technology, Louisiana State University, Baton Rouge, LA (jgaray@lsu.edu).

‡Université Paris-Saclay, CentraleSupélec, 3 rue Joliot-Curie, 91190 Gif-sur-Yvette, France, and Faculty of Engineering and Information Technology, University of Pécs, H-7622 Pécs, Vasvári Pál utca 4, Hungary (frederic.magoules@hotmail.com).

§Department of Mathematics, Temple University, Philadelphia, PA (szyld@temple.edu).

approximation of the Steklov-Poincaré operator by using differential operators [11, 20, 29]. The simplest of such an approximation is called OO0, and Λ is the zeroth-order approximation of the Steklov-Poincaré operator, i.e., $\Lambda = \alpha$, where α is a constant. In other words, this boundary condition is of Robin type. Since the convergence factor of the method (usually the spectral radius of the iteration operator) depends on the value of this parameter α, in optimized Schwarz methods one tunes the value of this boundary parameter to improve the convergence with respect to the classical Schwarz case ($\alpha = \infty$).

We are exploring the use of optimized Schwarz methods as outer solvers for the solution of PDEs. These types of outer solvers are fast and can be implemented asynchronously; see [21, 33]. In this paper, we analyze the convergence properties of an asynchronous optimized Schwarz method at the continuous level applied as a solver for Poisson's equation *in a bounded rectangular domain* with Dirichlet (physical) boundary conditions.

In [10], a convergence analysis of the classical Schwarz method is presented for a bounded domain with multiple subdomains, for the case in which the subdomains form a one-way partition of the domain and in which each overlapped region is shared by two subdomains. See also [14] for an analysis of optimized Schwarz methods for Poisson's equation in a rectangular domain using a one-way subdivision of the domain. In [22] we presented a preliminary analysis of the convergence of the optimized Schwarz method in the synchronous case for a problem defined in a bounded domain and for an arbitrary number of subdomains, when the subdomains form a two-dimensional subdivision containing cross points. In this paper, a more detailed version of that analysis is presented, and the analysis is extended to include the asynchronous case.

We mention that the analysis of the synchronous (and asynchronous) optimized Schwarz iterations in [21, 33] is based on Fourier transforms, and the synchronous method can be expressed as a linear map from the coefficients representing the Fourier transform at the nth iteration to those at the $(n+1)$st iteration. Such linear map can be represented by a matrix (of finite order, usually of order $2p$, for p subdomains or strips). Thus, for this finite-dimensional operator one can use results for the analysis of asynchronous iterations such as those in [7, 9, 15] (see also [19]). In [17] and [35] the convergence conditions for the asynchronous iterations is extended to infinite-dimensional operators. Here, for the decomposition with cross points, we need to use a different approach, and we obtain an infinite-dimensional operator $\hat{T}$. For our convergence proof of the asynchronous method for the infinite-dimensional operator, we create special infinite-dimensional boxes so that the hypotheses of the convergence theorem from [7] are satisfied.

Our contribution is manifold. We use a *generalized Fourier series* to represent each of the four components of the error of the synchronous optimized Schwarz iterations for the rectangular subdomains with cross-points (see Section 4). This representation is substantially different and more difficult to obtain than the use of a Fourier transform (which cannot be applied in this case). We prove that these series converge uniformly and that we can interchange the order of the summation and the derivatives. In this manner we can show that these series indeed represent the error of the synchronous (or asynchronous) iterations. A lot of the work consists of analyzing the nature of these series. These results allow us to write the synchronous iteration as a map $\hat{T}$ from the coefficients of these series at iteration n to the coefficients at iteration $n+1$. We approximate this infinite-dimensional operator by considering an appropriate truncation of the generalized Fourier series and the finite-dimensional operator $\hat{T}_{k_{\max}}$ that maps the vectors containing the coefficients of the truncated series from step n to step $n+1$; see the definition of these operators in Section 4. We prove convergence results using appropriate hypotheses on the finite-dimensional operators $\hat{T}_{k_{\max}}$, $k_{\max} \in \mathbb{N}$, for the synchronous case and on the infinite-dimensional operator $\hat{T}$ for the asynchronous case

(Sections 4 and 6) and show numerically that for certain configurations of the subdomains these hypotheses hold. In fact, it is computationally very inexpensive to test these hypotheses. In addition, we provide empirically the optimal value of the Robin parameter α as a function of the problem parameters (Section 8).

We mention here that our convergence results, both in the synchronous (Section 4) and asynchronous settings (Section 6), are the first such proofs for the case of a rectangular (bounded) domain with cross-points, with the exception of the preliminary summarized exposition in our conference paper [22].

One way to look at our contribution is that we took a very hard problem (convergence analysis on a bounded domain with cross points), and by considering the problem at the continuous level and proving an appropriate convergence theorem, we transformed it into a simple computational problem. Namely, examining the spectral radius of a small matrix, whose order is not related to the number of degrees of freedom of the discretized PDE. Furthermore, in this manner it is possible to analyze the effect of the parameters of the domain decomposition (amount of overlap, number of subdomains, size of the subdomains) on the bound of the convergence rate of the method.

Numerical experiments in Section 9 illustrate our theoretical results and complement the numerical results in [14, 33], showing that indeed asynchronous optimized Schwarz methods can be effective; see also [23]. Several appendices present detailed proofs of some of the results mentioned in the paper. By postponing some of the proofs to the end of the paper, we hope that the reader can capture its essence without being distracted by the technical details.

2. Formulation of the problem. We want to solve Poisson's equation in a rectangular domain subject to nonhomogeneous Dirichlet boundary conditions, i.e.,

$$\begin{cases} -\Delta u = f & \text{in } \Omega, \\ \quad u = g & \text{on } \partial\Omega, \end{cases} \tag{2.1}$$

where $\Omega = [0, L_1] \times [0, L_2]$.

We divide the physical domain into $p \times q$ overlapping rectangular subdomains. To simplify the presentation, we consider square subdomains where each side is of length H and we have the same overlap on each side, but the analysis presented here can easily be extended to arbitrary rectangles and an arbitrary amount of overlap (as long as the overlap does not cover the whole subdomain—a minimal assumption). Each of these subdomains is represented by a pair of indexes, (s, r), with $s \in \{1, \ldots, p\}$ and $r \in \{1, \ldots, q\}$. Let h be the length of the side of each interior square subdomain (i.e., subdomains not touching the physical boundary) as if it were a partition with no overlap. That is, by shrinking each of the overlapping subdomains by the amount γ on each side which is not a boundary of Ω, we obtain the nonoverlapping subdomains which form a partition of Ω. We have then overlapping square subdomains with side $H = h + 2\gamma$ and can use γ as a parameter to quantify the amount of overlap between subdomains; see Figure 2.1. We will later use a normalized value of this overlap, namely $\bar{\gamma} = \gamma/H$.

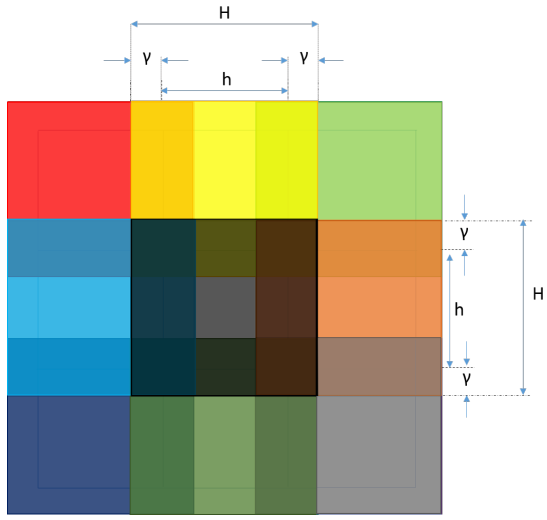

FIG. 2.1. *Example of a* 3×3 *decomposition of a square domain.*

The optimized Schwarz (OS) iteration process associated with problem (2.1) and with $OO0$ transmission conditions is defined, for an interior subdomain (i.e., for $1 < s < p$, $1 < r < q$), by

$$
\text{(2.2)} \qquad \begin{cases}
-\Delta u_{n+1}^{(s,r)} = f & \text{in } \Omega^{(s,r)}, \\
-\dfrac{\partial u_{n+1}^{(s,r)}}{\partial x} + \alpha u_{n+1}^{(s,r)} = -\dfrac{\partial u_{n}^{(s-1,r)}}{\partial x} + \alpha u_{n}^{(s-1,r)} & \text{for } x = (s-1)h - \gamma, \\
\dfrac{\partial u_{n+1}^{(s,r)}}{\partial x} + \alpha u_{n+1}^{(s,r)} = \dfrac{\partial u_{n}^{(s+1,r)}}{\partial x} + \alpha u_{n}^{(s+1,r)} & \text{for } x = sh + \gamma, \\
-\dfrac{\partial u_{n+1}^{(s,r)}}{\partial y} + \alpha u_{n+1}^{(s,r)} = -\dfrac{\partial u_{n}^{(s,r-1)}}{\partial y} + \alpha u_{n}^{(s,r-1)} & \text{for } y = (r-1)h - \gamma, \\
\dfrac{\partial u_{n+1}^{(s,r)}}{\partial y} + \alpha u_{n+1}^{(s,r)} = \dfrac{\partial u_{n}^{(s,r+1)}}{\partial y} + \alpha u_{n}^{(s,r+1)} & \text{for } y = rh + \gamma,
\end{cases}
$$

where $\frac{\partial}{\partial x}$ and $\frac{\partial}{\partial y}$ are, in this instance, normal derivatives[1]. The parameter α is the one that we want to tune to minimize the bound for the convergence rate. The subdomains touching the boundaries have one or two boundaries that are actually physical (not artificial) boundaries. The equations for the subdomains touching the boundaries are similar to (2.2) with the exception that one or two of the boundary conditions are Dirichlet, namely the ones associated with the physical boundaries.

Equation (2.2) simply says that we solve the local problem (in $\Omega^{(s,r)}$) with Robin boundary conditions, using as boundary values from the neighboring subdomains the iterates from the previous iteration.

We want to study the convergence of the OS iteration represented by (2.2) and the analogous equations for subdomains touching the boundaries. To that end, let us define the error $\eta_n = u_n - u_*$, where u_* is the solution of (2.1). Thus, the error $\eta_n^{(s,r)}$ is the nth iterate

[1]As mentioned in the introduction, the usual formulation of the OO0 condition is with the normal derivative across the artificial interfaces.

of (2.2), with $f = 0$, for the interior subdomains. We have that $\eta_n = (\eta_n^{(1,1)}, \ldots, \eta_n^{(p,q)})$. A convergence analysis of the OS iteration is therefore equivalent to analyzing the convergence to zero of each of the errors $\eta_n^{(s,r)}$. The plan is to write the restriction of the error to each subdomain in terms of a set of generalized Fourier series and then recast the OS iteration (with $f = 0$ and $g = 0$) as an iteration for the (infinite) vector containing the coefficients of these generalized Fourier series.

3. Recasting the OS iteration as a new fixed point iteration. To obtain the new formulation, we begin by analyzing the local error in an interior subdomain. Let $\eta_n^{(s,r)}$ be the local error after n iterations corresponding to the subdomain (s, r). As already mentioned, by linearity, we can see that the local error for the interior subdomains of the iteration process is described by (2.2) with $f = 0$. Furthermore, following a standard approach as described, e.g., in [24], by the superposition principle we can write $\eta_n^{(s,r)} = \eta_{n,1}^{(s,r)} + \eta_{n,2}^{(s,r)} + \eta_{n,3}^{(s,r)} + \eta_{n,4}^{(s,r)}$, where $\eta_{n,i}^{(s,r)}$, $i = 1, \ldots, 4$, is the solution of (2.2) with $f = 0$ and with one nonhomogeneous boundary condition and the rest homogeneous. We use the following convention: $i = 1$ corresponds to the case where the non-homogeneous boundary condition is at the bottom, $i = 2$ to the case with non-homogeneous boundary condition on the right, $i = 3$ at the top, and $i = 4$ on the left. To distinguish between the global variables (x, y), which are Cartesian coordinates with respect to the origin placed at the bottom left corner of Ω, and local variables, which are Cartesian coordinates within each subdomain with the origin coinciding with the bottom left corner of

$$\Omega^{(s,r)} = [(s-1)(H-2\gamma), sH - 2(s-1)\gamma] \times [(r-1)(H-2\gamma), rH - 2(r-1)\gamma],$$

considered as the square $(0, H)^2$, we denote the latter by (x_ℓ, y_ℓ). Thus, the relation between the local coordinates, denoted by (x_ℓ, y_ℓ), and the global coordinates, denoted by (x, y), is given by the following formulas:

$$x_\ell = x - (s-1)(H-2\gamma), \qquad y_\ell = y - (r-1)(H-2\gamma). \tag{3.1}$$

With this notation, we can explicitly write the equations for each of the four components of the error as follows.

$$\left\{\begin{array}{rl}
-\Delta\eta_{n+1,1}^{(s,r)} = 0 & \text{in } (0,H)^2, \\
-\dfrac{\partial\eta_{n+1,1}^{(s,r)}}{\partial x_\ell} + \alpha\eta_{n+1,1}^{(s,r)} = 0 & \text{for } x_\ell = 0, \\
\dfrac{\partial\eta_{n+1,1}^{(s,r)}}{\partial x_\ell} + \alpha\eta_{n+1,1}^{(s,r)} = 0 & \text{for } x_\ell = H, \\
\left(-\dfrac{\partial\eta_{n+1,1}^{(s,r)}}{\partial y_\ell} + \alpha\eta_{n+1,1}^{(s,r)}\right)(x_\ell, y_\ell) = \left(-\dfrac{\partial\eta_n^{(s,r-1)}}{\partial y_\ell} + \alpha\eta_n^{(s,r-1)}\right)(x_\ell, H-2\gamma) & \text{for } y_\ell = 0, \\
\dfrac{\partial\eta_{n+1,1}^{(s,r)}}{\partial y_\ell} + \alpha\eta_{n+1,1}^{(s,r)} = 0 & \text{for } y_\ell = H,
\end{array}\right. \tag{3.2}$$

ETNA
Kent State University and
Johann Radon Institute (RICAM)

$$
\left\{
\begin{array}{rl}
-\Delta \eta_{n+1,2}^{(s,r)} = 0 & \text{in } (0,H)^2, \\
-\dfrac{\partial \eta_{n+1,2}^{(s,r)}}{\partial x_\ell} + \alpha \eta_{n+1,2}^{(s,r)} = 0 & \text{for } x_\ell = 0, \\
\left(\dfrac{\partial \eta_{n+1,2}^{(s,r)}}{\partial x_\ell} + \alpha \eta_{n+1,2}^{(s,r)} \right)(x_\ell, y_\ell) = \left(\dfrac{\partial \eta_{n}^{(s+1,r)}}{\partial x_\ell} + \alpha \eta_{n}^{(s+1,r)} \right)(2\gamma, y_\ell) & \text{for } x_\ell = H, \\
-\dfrac{\partial \eta_{n+1,2}^{(s,r)}}{\partial y_\ell} + \alpha \eta_{n+1,2}^{(s,r)} = 0 & \text{for } y_\ell = 0, \\
\dfrac{\partial \eta_{n+1,2}^{(s,r)}}{\partial y_\ell} + \alpha \eta_{n+1,2}^{(s,r)} = 0 & \text{for } y_\ell = H,
\end{array}
\right. \tag{3.3}
$$

$$
\left\{
\begin{array}{rl}
-\Delta \eta_{n+1,3}^{(s,r)} = 0 & \text{in } (0,H)^2, \\
-\dfrac{\partial \eta_{n+1,3}^{(s,r)}}{\partial x_\ell} + \alpha \eta_{n+1,3}^{(s,r)} = 0 & \text{for } x_\ell = 0, \\
\dfrac{\partial \eta_{n+1,3}^{(s,r)}}{\partial x_\ell} + \alpha \eta_{n+1,3}^{(s,r)} = 0 & \text{for } x_\ell = H, \\
-\dfrac{\partial \eta_{n+1,3}^{(s,r)}}{\partial y_\ell} + \alpha \eta_{n+1,3}^{(s,r)} = 0 & \text{for } y_\ell = 0, \\
\left(\dfrac{\partial \eta_{n+1,3}^{(s,r)}}{\partial y_\ell} + \alpha \eta_{n+1,3}^{(s,r)} \right)(x_\ell, y_\ell) = \left(\dfrac{\partial \eta_{n}^{(s,r+1)}}{\partial y_\ell} + \alpha \eta_{n}^{(s,r+1)} \right)(x_\ell, 2\gamma) & \text{for } y_\ell = H,
\end{array}
\right. \tag{3.4}
$$

$$
\left\{
\begin{array}{rl}
-\Delta \eta_{n+1,4}^{(s,r)} = 0 & \text{in } (0,H)^2, \\
\left(-\dfrac{\partial \eta_{n+1,4}^{(s,r)}}{\partial x_\ell} + \alpha \eta_{n+1,4}^{(s,r)} \right)(x_\ell, y_\ell) = \left(-\dfrac{\partial \eta_{n}^{(s-1,r)}}{\partial x_\ell} + \alpha \eta_{n}^{(s-1,r)} \right)(H-2\gamma, y_\ell) & \text{for } x_\ell = 0, \\
\dfrac{\partial \eta_{n+1,4}^{(s,r)}}{\partial x_\ell} + \alpha \eta_{n+1,4}^{(s,r)} = 0 & \text{for } x_\ell = H, \\
-\dfrac{\partial \eta_{n+1,4}^{(s,r)}}{\partial y_\ell} + \alpha \eta_{n+1,4}^{(s,r)} = 0 & \text{for } y_\ell = 0, \\
\dfrac{\partial \eta_{n+1,4}^{(s,r)}}{\partial y_\ell} + \alpha \eta_{n+1,4}^{(s,r)} = 0 & \text{for } y_\ell = H.
\end{array}
\right. \tag{3.5}
$$

The benefit of splitting the error into four parts, where each part satisfies three homogeneous boundary conditions, is that the equations defining each part of the local error can be solved using separation of variables, leading to a series representation of each part of the error, where each term of the series is the product of two functions of one variable and their product is a harmonic function in 2D. Moreover, the explicit expressions of these functions are easily obtained by solving simple ODEs. In what follows we show how to construct these series for part 1 of the error in the interior subdomain (s,r), i.e., for $\eta_{n,1}^{(s,r)}$. The series representation of the other parts of the error can be obtained by a similar procedure, and it is therefore omitted for brevity.

The goal is to write the solution of each component of the error, i.e., the solutions of the equations (3.2)–(3.5) as generalized Fourier series in one of the variables while the other variable remains fixed. Each term of such series contains a product of two functions. These functions are solutions of certain ODEs, which we describe now.

Let ϕ_m be the solution of

$$\begin{cases} \dfrac{d^2\phi_m}{dx_\ell^2}(x_\ell) + (\dfrac{z_m}{H})^2\phi_m(x_\ell) = 0 & \text{for } x_\ell \in (0,H), \\ -\dfrac{d\phi_m}{dx_\ell}(x_\ell) + \alpha\phi_m(x_\ell) = 0 & \text{for } x_\ell = 0, \\ \dfrac{d\phi_m}{dx_\ell}(x_\ell) + \alpha\phi_m(x_\ell) = 0 & \text{for } x_\ell = H, \end{cases} \tag{3.6}$$

and let ψ_m be the solution of

$$\begin{cases} \dfrac{d^2\psi_m}{dx_\ell^2}(y_\ell) - (\dfrac{z_m}{H})^2\psi_m(y_\ell) = 0 & \text{for } y_\ell \in (0,H), \\ -\dfrac{d\psi_m}{dx_\ell}(y_\ell) + \alpha\psi_m(y_\ell) = 0 & \text{for } y_\ell = 0. \end{cases} \tag{3.7}$$

Then, we have that the solutions of these systems are

$$\phi_m(x_\ell) = \frac{\bar{\alpha}}{z_m}\sin\left(\frac{z_m x_\ell}{H}\right) + \cos\left(\frac{z_m x_\ell}{H}\right) \tag{3.8}$$

and

$$\psi_m(y_\ell) = \frac{\bar{\alpha}}{z_m}\sinh\left(\frac{z_m y_\ell}{H}\right) + \cosh\left(\frac{z_m y_\ell}{H}\right), \tag{3.9}$$

where $\{z_m\}_{m\in\mathbb{N}}$ is the set of solutions of the transcendental equation

$$(\bar{\alpha}^2 - z^2)\sin(z) - (2z\bar{\alpha})\cos(z) = 0 \tag{3.10}$$

and labeled so that

$$z_1 < z_2 < \cdots \tag{3.11}$$

and where $\bar{\alpha} = \alpha H$ is the “normalized" Robin parameter, i.e., the Robin parameter times the width of the subdomain.

We begin by observing that the product of these functions is harmonic. The proof of the following lemma is given in Appendix A.

LEMMA 3.1. *The function* $v_m : [0,1]^2 \to \mathbb{R}$ *defined as*

$$v_m(x_\ell, y_\ell) = \phi_m(x_\ell)\psi_m(H - y_\ell) \tag{3.12}$$

is harmonic.

As a consequence, we have that the function (3.12) satisfies Laplace's equation in $(0,H)^2$ and the three homogeneous boundary conditions in (3.2). Given that Laplace's equation and these boundary conditions are homogeneous, by the superposition principle we have that any linear combination of $\{\phi_m(x_\ell)\psi_m(H - y_\ell)\}$ also satisfies Laplace's equation and the homogeneous boundary conditions. Then, the series

$$\sum_{m=1}^{\infty} A_m\phi_m(x_\ell)\psi_m(H - y_\ell)$$

also satisfies these equations provided that the order of infinite summation and differentiation commutes. In Theorem 3.2 we show that the series

$$v(x_\ell, y_\ell) = \sum_{m=1}^{\infty} \frac{B_m}{z_m^{5/2}} \phi_m(x_\ell)\psi_m(H - y_\ell) \tag{3.13}$$

satisfies (3.2) with the appropriate choice of $\{B_m\}_{m\in\mathbb{N}}$. The reason for writing the series (3.13) in that form is to show that, given that $\{\phi_m\}_{m\in\mathbb{N}}$ and $\{\psi_m/\psi_m(H)\}_{m\in\mathbb{N}}$ are uniformly bounded in $(0, H)$, if $\{B_m\}_{m\in\mathbb{N}}$ is uniformly bounded, then the terms of the series decay at least as fast as $1/z_m^{5/2}$. As shown in Lemma B.1 in Appendix B, this rate of decay of the terms of the series is enough to ensure that the order of summation and differentiation commutes for that series.

We also comment on the hypotheses of Theorem 3.2 below, whose proof is given in Appendix C. One of them is that the initial error η_0 is piecewise C^3 in Ω. Note that when $f \in C^1(\Omega)$ we have $u_* \in C^3(\Omega)$. Then, the condition $\eta_0 \in C^3(\Omega)$ is easily obtained, for example, with $u_0 = 0$. The other is that $2\gamma < H$, that is, that the overlapped regions do not cover the whole subdomain. This is of course very natural, and in practice it is not a real restriction.

Observe that (3.6) is a regular Sturm-Liouville eigenvalue problem with eigenvalues $\lambda_m = (z_m/H)^2$. By the Sturm-Liouville theory, $\{\phi_m\}_{m\in\mathbb{N}}$ is a complete orthogonal set in $[0, H]$; see, e.g., [24, pp. 174–178]. Therefore, the expression (3.13) can be seen as a generalized Fourier series in the x_ℓ-variable. In Theorem 3.2 we use the orthogonality of $\{\phi_m\}_{m\in\mathbb{N}}$ to determine the values of the coefficients B_m. Recall that one of the benefits of expanding the error parts as linear combinations of the product $\phi_m\psi_m$ is that this product is harmonic and therefore any truncation of the series (3.13) is also harmonic.

THEOREM 3.2. *Let u_0 be the initial approximation of the solution of (2.1) and such that the initial error $\eta_0 = u_0 - u_*$ is piecewise C^3 in Ω. Assume further that the overlap γ is small enough so that $2\gamma < H$. Then, the four parts of the local error of the interior subdomains can be written as*

$$\eta_{n,1}^{(s,r)}(x_\ell, y_\ell) = \sum_{m=1}^{\infty} \frac{B_{n,m,1}^{(s,r)}}{z_m^{5/2}\psi_m(H)} \phi_m(x_\ell)\psi_m(H - y_\ell)\ , \tag{3.14}$$

$$\eta_{n,2}^{(s,r)}(x_\ell, y_\ell) = \sum_{m=1}^{\infty} \frac{B_{n,m,2}^{(s,r)}}{z_m^{5/2}\psi_m(H)} \phi_m(y_\ell)\psi_m(x_\ell)\ , \tag{3.15}$$

$$\eta_{n,3}^{(s,r)}(x_\ell, y_\ell) = \sum_{m=1}^{\infty} \frac{B_{n,m,3}^{(s,r)}}{z_m^{5/2}\psi_m(H)} \phi_m(x_\ell)\psi_m(y_\ell)\ , \tag{3.16}$$

$$\eta_{n,4}^{(s,r)}(x_\ell, y_\ell) = \sum_{m=1}^{\infty} \frac{B_{n,m,4}^{(s,r)}}{z_m^{5/2}\psi_m(H)} \phi_m(y_\ell)\psi_m(H - x_\ell)\ , \tag{3.17}$$

where ϕ_m and ψ_m are given by (3.8) and (3.9), respectively, and

$$|B_{n,m,i}^{(s,r)}| \le M_n^{(s,r)} \tag{3.18}$$

for all $m \in \mathbb{N}$ and some $M_n^{(s,r)} > 0$.

We note that (3.14) and (3.16) are generalized Fourier series in the variable x_ℓ, while (3.15) and (3.17) are generalized Fourier series in the variable y_ℓ.

Theorem 3.2 provides explicit series expansions of each part of the error in the interior subdomains. The corresponding series expansions of the different parts of the errors in

subdomains not in the interior, i.e., those along the boundaries of the domain Ω have a similar form, but the functions involved are a little different, precisely to account for the values at the boundary. For completeness, they are presented in detail in the following.

The functions for the generalized Fourier series for subdomains on the boundary are $\phi_m^{(b)}$, the solutions of

$$\begin{cases} \dfrac{d^2\phi_m^{(b)}}{dx_\ell^2}(x) + (\dfrac{\tilde{z}_m}{H})^2\phi_m^{(b)}(x) = 0 & \text{for } x \in (0, H), \\ \phi_m^{(b)}(x) = 0 & \text{for } x = 0, \\ \dfrac{d\phi_m^{(b)}}{dx_\ell}(x) + \alpha\phi_m^{(b)}(x) = 0 & \text{for } x = H, \end{cases}$$

and the functions $\psi_m^{(b)}$ which solve

$$\begin{cases} \dfrac{d^2\psi_m^{(b)}}{dx_\ell^2}(x) - (\dfrac{\tilde{z}_m}{H})^2\psi_m^{(b)}(x) = 0 & \text{for } x \in (0, H), \\ \psi_m^{(b)}(x) = 0 & \text{for } x = 0. \end{cases}$$

The solution of these systems are

$$\psi_m^{(b)}(x) := \sinh\left(\frac{\tilde{z}_m x}{H}\right) \tag{3.19}$$

and

$$\phi_m^{(b)}(x) := \sin\left(\frac{\tilde{z}_m x}{H}\right), \tag{3.20}$$

where $\{\tilde{z}_m\}_{m\in\mathbb{N}}$ are such that $\tilde{z}_1 < \tilde{z}_2 < \cdots$ and $\tilde{z}_m$ satisfies the transcendental equation

$$\bar{\alpha}\sin(\tilde{z}) + \tilde{z}\cos(\tilde{z}) = 0\,. \tag{3.21}$$

As was the case for the basis functions for the interior subdomains $\{\phi_m\}$, the set of these new basis functions $\{\phi_m^{(b)}\}$ is a complete orthogonal set in $[0, H]$ that spans the set of piecewise continuous functions. For subdomains on the corners, two of the boundary conditions are already homogeneous (zero Dirichlet boundary conditions). Thus, we only have two non-homogeneous boundary conditions in this case, and therefore we only need to divide the error of the corner subdomains into two parts (i.e., if we split the error in four parts, two of them are zero). However, we will keep the same convention for the values of the index i as before. Thus, for the subdomain on the bottom-left corner we have that $i = 2, 3$, which means that we only have non-homogeneous boundary conditions on the right and top sides of the subdomain. Using separation of variables and the superposition principle, the series expansion of the parts of the local errors of the corner subdomains at the nth iteration can be written as

$$\begin{aligned} \eta_n^{(1,q)}(x_\ell, y_\ell) = &\sum_{m=1}^{\infty} \frac{(\bar{\alpha} + 1/\tilde{z}_m)B_{n,m,1}^{(1,q)}}{\tilde{z}_m^{5/2}\cosh(\tilde{z}_m)}\phi_m^{(b)}(x_\ell)\psi_m^{(b)}(y_\ell - H) \\ &+ \sum_{m=1}^{\infty} \frac{(\bar{\alpha} + 1/\tilde{z}_m)B_{n,m,2}^{(1,q)}}{\tilde{z}_m^{5/2}\cosh(\tilde{z}_m)}\phi_m^{(b)}(y_\ell - H)\psi_m^{(b)}(x_\ell), \end{aligned} \tag{3.22}$$

$$\begin{aligned}\eta_n^{(p,q)}(x_\ell,y_\ell) &= \sum_{m=1}^{\infty}\frac{(\bar\alpha+1/\tilde z_m)B_{n,m,1}^{(p,q)}}{\tilde z_m^{5/2}\cosh(\tilde z_m)}\phi_m^{(b)}(x_\ell-H)\psi_m^{(b)}(y_\ell-H)\\ &\quad+\sum_{m=1}^{\infty}\frac{(\bar\alpha+1/\tilde z_m)B_{n,m,4}^{(p,q)}}{\tilde z_m^{5/2}\cosh(\tilde z_m)}\psi_m^{(b)}(x_\ell-H)\phi_m^{(b)}(y_\ell-H),\end{aligned}\tag{3.23}$$

$$\begin{aligned}\eta_n^{(p,1)}(x_\ell,y_\ell) &= \sum_{m=1}^{\infty}\frac{(\bar\alpha+1/\tilde z_m)B_{n,m,3}^{(p,1)}}{\tilde z_m^{5/2}\cosh(\tilde z_m)}\phi_m^{(b)}(x_\ell-H)\psi_m^{(b)}(y_\ell)\\ &\quad+\sum_{m=1}^{\infty}\frac{(\bar\alpha+1/\tilde z_m)B_{n,m,4}^{(p,1)}}{\tilde z_m^{5/2}\cosh(\tilde z_m)}\psi_m^{(b)}(x_\ell-H)\phi_m^{(b)}(y_\ell),\end{aligned}\tag{3.24}$$

$$\begin{aligned}\eta_n^{(1,1)}(x_\ell,y_\ell) &= \sum_{m=1}^{\infty}\frac{(\bar\alpha+1/\tilde z_m)B_{n,m,2}^{(1,1)}}{\tilde z_m^{5/2}\cosh(\tilde z_m)}\psi_m^{(b)}(x_\ell)\phi_m^{(b)}(y_\ell)\\ &\quad+\sum_{m=1}^{\infty}\frac{(\bar\alpha+1/\tilde z_m)B_{n,m,3}^{(1,1)}}{\tilde z_m^{5/2}\cosh(\tilde z_m)}\phi_m^{(b)}(x_\ell)\psi_m^{(b)}(y_\ell).\end{aligned}\tag{3.25}$$

We need these new functions $\phi_m^{(b)}$ and $\psi_m^{(b)}$ because, unlike for the interior subdomains case where all of the boundary conditions are of Robin type, in the case of subdomains touching the boundary, there are mixed boundary conditions, where on some sides they are of Dirichlet type and on the others they are of Robin type. The series representation of the local errors of the subdomains touching the boundary that are not corners (i.e., on the sides) at the nth iteration are

$$\begin{aligned}\eta_n^{(1,r)}(x_\ell,y_\ell) &= \sum_{m=1}^{\infty}\frac{B_{n,m,1}^{(1,r)}}{\tilde z_m^{5/2}\psi_m(H)}\phi_m^{(b)}(x_\ell)\psi_m(H-y_\ell)\\ &\quad+\sum_{m=1}^{\infty}\frac{B_{n,m,2}^{(1,r)}}{z_m^{5/2}\cosh(\tilde z_m)}\phi_m(y_\ell)\psi_m^{(b)}(x_\ell)\\ &\quad+\sum_{m=1}^{\infty}\frac{B_{n,m,3}^{(1,r)}}{\tilde z_m^{5/2}\psi_m(H)}\phi_m^{(b)}(x_\ell)\psi_m(y_\ell),\end{aligned}\tag{3.26}$$

$$\begin{aligned}\eta_n^{(p,r)}(x_\ell,y_\ell) &= \sum_{m=1}^{\infty}\frac{B_{n,m,1}^{(p,r)}}{\tilde z_m^{5/2}\psi_m(H)}\phi_m^{(b)}(x_\ell-H)\psi_m(H-y_\ell)\\ &\quad+\sum_{m=1}^{\infty}\frac{B_{n,m,3}^{(p,r)}}{\tilde z_m^{5/2}\psi_m(H)}\phi_m^{(b)}(x_\ell-H)\psi_m(y_\ell)\\ &\quad+\sum_{m=1}^{\infty}\frac{B_{n,m,4}^{(p,r)}}{z_m^{5/2}\cosh(\tilde z_m)}\phi_m(y_\ell)\psi_m^{(b)}(x_\ell-H),\end{aligned}\tag{3.27}$$

$$\begin{aligned}\eta_n^{(s,1)}(x_\ell,y_\ell) &= \sum_{m=1}^{\infty}\frac{B_{n,m,4}^{(s,1)}}{\tilde z_m^{5/2}\psi_m(H)}\phi_m^{(b)}(y_\ell)\psi_m(H-x_\ell)\\ &\quad+\sum_{m=1}^{\infty}\frac{B_{n,m,2}^{(s,1)}}{z_m^{5/2}\cosh(\tilde z_m)}\phi_m^{(b)}(y_\ell)\psi_m^{(b)}(x_\ell)\\ &\quad+\sum_{m=1}^{\infty}\frac{B_{n,m,3}^{(s,1)}}{\tilde z_m^{5/2}\cosh(\tilde z_m)}\phi_m(x_\ell)\psi_m^{(b)}(y_\ell),\end{aligned}\tag{3.28}$$

$$\begin{aligned}\eta_n^{(s,q)}(x_\ell, y_\ell) = &\sum_{m=1}^{\infty} \frac{B_{n,m,1}^{(s,q)}}{\tilde{z}_m^{5/2}\cosh(\tilde{z}_m)}\phi_m(x_\ell)\psi_m^{(b)}(H-y_\ell) \\ &+ \sum_{m=1}^{\infty} \frac{B_{n,m,2}^{(s,q)}}{\tilde{z}_m^{5/2}\psi_m(H)}\phi_m^{(b)}(y_\ell - H)\psi_m(x_\ell) \\ &+ \sum_{m=1}^{\infty} \frac{B_{n,m,4}^{(s,q)}}{z_m^{5/2}\psi_m(H)}\phi_m^{(b)}(H-y_\ell)\psi_m(H-x_\ell).\end{aligned} \tag{3.29}$$

We pause here to note that the expressions of the errors at the nth iteration in each of the $p \times q$ subdomains described by the series (3.14)–(3.17), (3.22)–(3.29), can be written in an encompassing manner as a series of the form

$$\eta_n^{(s,r)}(x_\ell, y_\ell) = \sum_{i=1}^{4}\sum_{m=1}^{\infty} B_{n,m,i}^{(s,r)}\varphi_{m,i}^{(s,r)}(x_\ell, y_\ell; \bar{\alpha}, H, z_m, \tilde{z}_m), \tag{3.30}$$

where the functions $\varphi_{m,i}^{(s,r)}$ depend also on the parameters $\bar{\alpha}$, H, and on either z_m, the solutions of equation (3.10), or $\tilde{z}_m$, the solutions of equation (3.21), and these series converge uniformly. In fact, the expression (3.30) can be seen simply as a shorthand for each of the expressions in (3.14)–(3.17), (3.22)–(3.29).

We are now ready to determine a new fixed point iteration which is equivalent to the optimized Schwarz method given by (2.2) together with the corresponding equations for the subdomains on the boundary. We want an operator mapping the vector of all the local error series coefficients at iteration n to the vector of coefficients at iteration $n+1$. To that end, plugging the series expansion of $\eta_{n+1,i}^{(s,r)}$ into its corresponding nonhomogeneous boundary conditions, multiplying both sides of the resulting equation by ϕ_k ($\phi_k^{(b)}$), integrating over $[0, H]$, and using the orthogonality property of the set $\{\phi_m\}_{m\in\mathbb{N}}$ $\left(\left\{\phi_m^{(b)}\right\}_{m\in\mathbb{N}}\right)$, we obtain[2] the expression of the error series coefficients at iteration $n+1$ in terms of those at iteration n. For interior subdomains that are not adjacent to subdomains touching the boundary, we have, for example, the expression for $B_{n+1,k,1}^{(s,r)}$ given in equation (C.16) in Appendix C. The formulas for the coefficients of the error series related to subdomains touching the boundary are similar.

We mention in passing that one can see in (C.16) that coefficients of frequency k at iteration $n+1$ depend not only on the coefficients of the error series at iteration n of frequency k, but also on the coefficients of other frequencies. In other words, this means that error modes of different frequencies are coupled. A phenomenon that does not occur when a one-way decomposition is used.

Let $\mathbf{B}_n$ be the infinite vector containing all the error series coefficients at iteration n, i.e., $\mathbf{B}_n = (b_1^{(n)}, b_2^{(n)}, \ldots)$ with

$$b_j^{(n)} \in \left\{B_{n,k,i}^{(s,r)} : s \in \{1,\ldots,p\},\, r \in \{1,\ldots,q\},\, k \in \mathbb{N}, i \in \{1,\ldots,4\}\right\}.$$

Then, the relation between the coefficients of the local errors can be written as

$$\mathbf{B}_{n+1} = \hat{T}\mathbf{B}_n,$$

[2]We develop these formulas using the program Mathematica.

where $\hat{T} : \mathbb{R}^\infty \to \mathbb{R}^\infty$ is an infinite matrix. The coupling between modes of different frequencies implies that every row of the infinite matrix $\hat{T}$ is nonzero. We can write this operator as $\hat{T} = [(\hat{T}^{(1,1)})^T, \ldots, (\hat{T}^{(p,q)})^T]^T$, where $\hat{T}^{(s,r)}$ is a local operator such that $\mathbf{B}_{n+1}^{(s,r)} = \hat{T}^{(s,r)}\mathbf{B}_n$ with $\mathbf{B}_{n+1}^{(s,r)}$ being a vector containing all the error series coefficients of the local problem (s, r) at iteration $(n + 1)$; see Figure 3.1. That is, we can think of this infinite matrix $\hat{T}$ as $p \times q$ block rows (of infinite size).

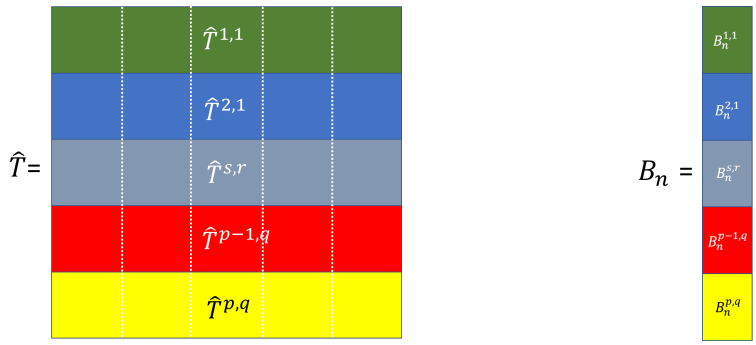

FIG. 3.1. *Schematic representation of the infinite matrix $\hat{T}$ and the vector $\mathbf{B}_n$.*

For the initial error η_0 we have

$$\Delta\eta_0 = \Delta u_0 - \Delta u_* = \Delta u_0 - f.$$

Note that the initial approximation u_0 need not be such that $\Delta u_0 = f$. Therefore, $\Delta\eta_0$ may not be harmonic. Then we cannot assume that $\eta_0^{(s,r)}$ can be written as a sum of the series (3.14)–(3.17), (3.22)–(3.29). However, after computing $u_1^{(s,r)}$ using the corresponding restriction of u_0 on the right-hand side of the corresponding local equations for the (s, r)-subdomain, we have that $\Delta u_1^{(s,r)} = f^{(s,r)}$, $\Delta\eta_1^{(s,r)} = 0$, and the error $\eta_1^{(s,r)}$ can be written in terms of the four parts given by the series (3.14)–(3.17), (3.22)–(3.29). From this it follows that we can represent η_1 by the vector $\mathbf{B}_1$. For $n \geq 1$ there is a one-to-one correspondence between η_n and $\mathbf{B}_n$. Hence, we can consider $\mathbf{B}_1$ as the starting point for the new fixed point iteration with the operator $\hat{T}$.

It follows then that in order to study the convergence of the optimized Schwarz method (2.2) and its asynchronous version defined later in Section 5, it suffices to study the properties of the operator $\hat{T}$. We have provided a general procedure of how to compute the coefficients of the operator $\hat{T}$. Each such coefficient is indexed by two indices, and each of these indices is determined by four numbers: the subdomain indices (s, r), with $s = 1, \ldots, p$, $r = 1, \ldots, q$, the index indicating which of the four parts of the errors we are considering, $i = 1, \ldots, 4$, and the mode $k = 1, 2, \ldots, \infty$, in the series expansion. For completeness, we provide in the rest of this section an explicit representation of the entries of this operator for the case of $1 < s < p$, $1 < r < q$. The cases of subdomains on the boundary of Ω are similar. Furthermore, since in some of our analysis we use a truncated version of this infinite operator $\hat{T}$, we develop an index system for that case as follows.

Consider the generalized Fourier series (3.14)–(3.17), (3.22)–(3.29) representing the errors at the nth iteration. Let us truncate each of them after $k_{\max}$ terms. Consider then the finite matrix $\hat{T}_{k_{\max}}$ which is the submatrix of $\hat{T}$ mapping the coefficients of these truncated series from the nth iteration to the $(n + 1)$st iteration. The vector $\mathbf{B}_n^{k_{\max}}$ is similarly truncated. The jth entry of the vector $\mathbf{B}_n^{k_{\max}}$ is denoted by $b_j^{(n)}$. We enumerate the error series

coefficients as entries of $\mathbf{B}_n^{k_{\max}}$ by pairing each coefficient with a global index. The global index $j = j(s, r, i, k, p, q)$ of the coefficient $B_{n,k,i}^{(s,r)}$ for a fixed value of $k_{\max}$ is given in the following expression.

$$
j = \begin{cases}
(i-2) * k_{\max} + k, \\
\qquad \text{if } (s,r) = (1,1), \\
(3 * (s-2) + i) * k_{\max} + k, \\
\qquad \text{if } 1 < s < p, r = 1, \\
(3 * (p-2) + i - 1) * k_{\max} + k, \\
\qquad \text{if } s = p, r = 1, \\
(4 + 3 * (p-2) + (6 + 4 * (p-2)) * (r-2) + (i-1)) * k_{\max} + k, \\
\qquad \text{if } s = 1, 1 < r < q, \\
(4 + 3 * (p-2) + (6 + 4 * (p-2)) * (r-2) + 3 + 4 * (s-2) + (i-1)) * k_{\max} + k, \\
\qquad \text{if } 1 < s < p, 1 < r < q, \\
(4 + 3 * (p-2) + (6 + 4 * (p-2)) * (r-2) + 3 + 4 * (p-2) + (\Psi(i,s,r,p,q) - 1)) * k_{\max} + k;, \\
\qquad \text{if } s = p, 1 < r < q, \\
(4 + 3 * (p-2) + (6 + 4 * (p-2)) * (q-2) + (i-1)) * k_{\max} + k, \\
\qquad \text{if } s = 1, r = q, \\
(4 + 3 * (p-2) + (6 + 4 * (p-2)) * (q-2) + 2 + 3 * (s-2) + (\Psi(i,s,r,p,q) - 1)) * k_{\max} + k, \\
\qquad 1 < s < p, r = q \\
(4 + 3 * (p-2) + (6 + 4 * (p-2)) * (q-2) + 2 + 3 * (p-2) + (i-1)/3) * k_{\max} + k, \\
\qquad s = p, r = q \\
10 * k_{\max} + (i-1) * k_{\max} + k, \\
\qquad p = 3, q = 3, s = 2, r = 2 \\
14 * k_{\max} + (i-1) * k_{\max} + k, \\
\qquad p = 3, q = 3, s = p, 1 < r < q,
\end{cases}
$$

where the function Ψ is given by

$$
\Psi(i,s,r,p,q) = \begin{cases}
1, & \text{if } s = p, i = 1, \\
2, & \text{if } s = p, i = 3, \\
3, & \text{if } s = p, i = 4, \\
1, & \text{if } r = q, i = 1, \\
2, & \text{if } r = q, i = 2, \\
3, & \text{if } r = q, i = 4.
\end{cases}
$$

The function Ψ takes the label of the index of the subdomain touching the boundary and returns the relative position among the active indexes for the given subdomain. It was introduced to identify the values of the index i for subdomains touching the boundary, given that for these subdomains i does not assume all the values of $\{1, 2, 3, 4\}$. For example, for the subdomains that are not corners and are touching the right boundary, i can only assume the values $1, 3$, or 4. For different values of $k_{\max}$, the vector has different lengths, and the indexing changes.

Thus, we have $\mathbf{B}_n^{k_{\max}} = (b_1^{(n)}, b_2^{(n)}, \ldots, b_\ell^{(n)})$, where $b_\ell^{(n)} = B_{n,m,i}^{(s,r)}$, for s, r, n, m, i such that $\ell = j(s, r, i, m, p, q)$. The $t_{l_{\hat{\mathrm{B}}}, l_{\hat{j}}}$-entry of $\hat{T}_{k_{\max}}$ is the factor that multiplies the coefficient $B_{n,\tilde{m},\tilde{i}}^{(\tilde{s},\tilde{r})}$ such that $j(\tilde{s}, \tilde{r}, \tilde{i}, \tilde{m}, p, q) = l_{\hat{j}}$ in the formula of the coefficient $B_{n+1,m,i}^{(s,r)}$ such that $j(s, r, i, m, p, q) = l_{\hat{\mathrm{B}}}$. Thus, the right-hand side of equation (C.16) with the summation indexes going from $m = 1$ to $m = k_{\max}$ can be seen as the result of multiplying the row of $\hat{T}_{k_{\max}}$ corresponding to the global index of $B_{n,k,1}^{(s,r)}$ and the vector $\mathbf{B}_n^{k_{\max}}$. Then, if $l_{\hat{\mathrm{B}}}$ is the global index of the coefficient $B_{n+1,k,1}^{(s,r)}$ from equation (C.16) and $l_{\hat{j}}$ is the global index of the coefficient $B_{n+1,m,2}^{(s,r)}$, then

$$t_{l_{\hat{\mathfrak{s}}},l_{\hat{\jmath}}} = \frac{4z_k^{11/2}\left[\frac{\bar{\alpha}}{z_k}\tanh(z_k)+1\right]\left(z_m+\frac{\bar{\alpha}^2}{z_m}\right)\sin\left((1-2\bar{\gamma})z_m\right)}{z_m^{1/2}\left[\left(z_k+\frac{\bar{\alpha}^2}{z_k}\right)\tanh(z_k)+2\bar{\alpha}\right]z_m^2\left(z_m z_k^3+z_k z_m^3\right)}$$
$$\times\frac{\left\{\tanh(z_m)\left[\bar{\alpha}(z_k^2+z_m^2)\sin(z_k)-z_k(\bar{\alpha}^2-z_m^2)\cos(z_k)\right]+z_m(\bar{\alpha}^2+z_k^2)\sin(z_k)\right\}}{\left[\frac{\bar{\alpha}}{z_m}\tanh(z_m)+1\right]\left[(z_k^2-\bar{\alpha}^2)\sin(2z_k)+2z_k(\bar{\alpha}^2+z_k^2+\bar{\alpha})-2\bar{\alpha}z_k\cos(2z_k)\right]}.$$

4. Convergence of the synchronous optimized Schwarz method. In this section we discuss the convergence of a synchronous implementation of the optimized Schwarz method described by (2.2) for the interior subdomains and similar equations describing the method for the subdomains on the boundary of Ω. The convergence result rely on the study of the spectral properties of a truncated version of the matrix $\hat{T}$, denoted $\hat{T}_{k_{\max}}$. Recall that $\hat{T}_{k_{\max}}$ is a finite matrix obtained by discarding the rows and columns of $\hat{T}$ corresponding to the coefficients pertaining to $k > k_{\max}$. Thus, $k_{\max}$ is the truncation parameter; the sparsity structure of $\hat{T}_{k_{\max}}$ is shown in Figure 4.1. Also, let us recall that $\mathbf{B}_n^{k_{\max}}$ is the truncated version of $\mathbf{B}_n$.

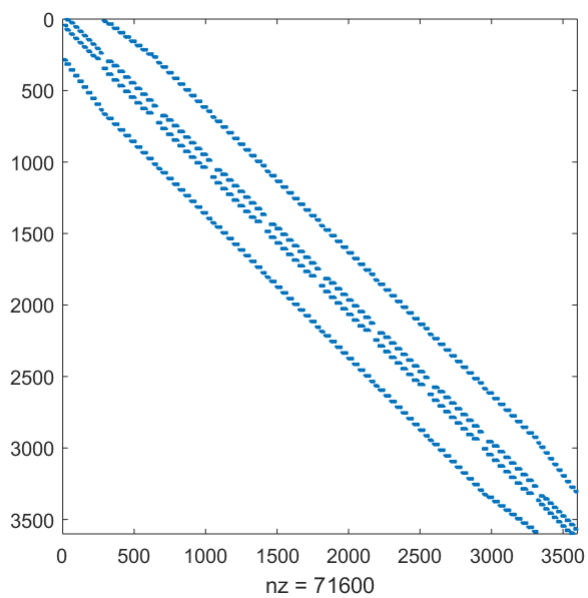

FIG. 4.1. *Sparsity structure of $\hat{T}_{k_{\max}}$ for $p = q = 10$ and $k_{max} = 10$.*

THEOREM 4.1. *Consider the synchronous optimized Schwarz iteration described by (2.2) and the analogous equations corresponding to subdomains touching the boundaries. Let us write the error parts as in (3.14)–(3.17) and (3.22)–(3.29). Let $\mathbf{B}_n$ be the vector whose entries are the coefficients of the error series from all subdomains at iteration n and $\hat{T}$ the infinite matrix described in Section 3 such that $\mathbf{B}_{n+1} = \hat{T}\mathbf{B}_n$. The matrix $\hat{T}_{k_{\max}}$ is a finite matrix obtained by discarding the rows and columns of $\hat{T}$ corresponding to the coefficients pertaining to $k > k_{\max}$. Let us denote by $\lambda_j^{k_{\max}}$ the jth eigenvalue of $\hat{T}_{k_{\max}}$, where we have ordered them in non-increasing order according to their modulus, and by $v_j^{k_{\max}}$ the corresponding eigenvectors normalized to have max-norm one. We assume that $\hat{T}_{k_{\max}}$ has a complete set of*

eigenvectors. Also, let us denote by $\mathbf{B}_n^{k_{\max}}$ *the truncated version of* $\mathbf{B}_n$*, which conforms to the truncation* $\hat{T}_{k_{\max}}$ *of* $\hat{T}$*.*

Then, the synchronous optimized Schwarz iteration converges for any initial u_0 *such that* $\eta_0 = u_0 - u_*$ *is piecewise* C^3 *in* Ω*, provided that the following two conditions hold.*

1. *The absolute values of* $\lambda_j^{k_{\max}}$ *form a non-increasing sequence that decreases fast enough so that there exists an* $\epsilon > 0$ *and an* $n_\epsilon \in \mathbb{N}$ *such that for* $n \geq n_\epsilon$ *we have* $|\lambda_j^{k_{\max}}|^n \leq 1/j^{(1+\epsilon)}$ *for all values of* $k_{\max} \in \mathbb{N}$*.*
2. *There exists* $0 < \rho < 1$ *such that the spectral radius* $\rho(\hat{T}_{k_{\max}}) \leq \rho$ *for all* $k_{\max} \in \mathbb{N}$*.*

The proof of Theorem 4.1 is given in Appendix E.

We make several remarks on the hypotheses of Theorem 4.1. Hypothesis 1 refers to the absolute value of the eigenvalues and their decay rate. We have observed that this hypothesis holds for all cases that we analyzed numerically. In Figure 4.2 this can be clearly observed. Note that instead of $|\lambda_j|$, we plot its value to the 30th power in a log-log plot.

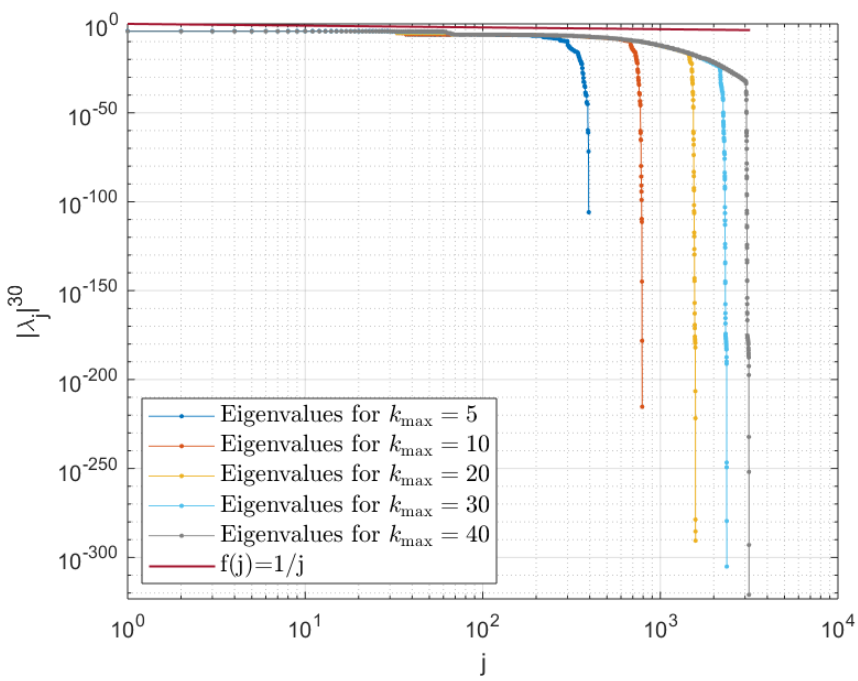

FIG. 4.2. *30th power of the absolute values of the eigenvalues of* $\hat{T}_{k_{\max}}$ *in non-increasing order for different values of* $k_{\max}$*,* $p = q = 5$*, and* $\bar{\gamma} = 0.01$*, and* $f(j) = 1/j$ *(in red).*

Hypothesis 2 refers to the spectral radius of the truncated matrix $\hat{T}_{k_{\max}}$. In all our computations, we have found that indeed $\rho(\hat{T}_{k_{\max}})$ is uniformly bounded for all values of $k_{\max}$ and that this bound is less than one for all values of the overlap larger than a minimum overlap. This is illustrated in Figure 4.3. Note that in fact $\rho(\hat{T}_{k_{\max}})$ is essentially constant for varying values of $k_{\max}$.

Furthermore, the two graphs in Figure 4.4 illustrate that the use of the spectral radius of the truncated matrices $\hat{T}_{k_{\max}}$ to characterize the convergence of the optimized restricted additive Schwarz (ORAS) method is valid. In this figure, we present the spectral radius of

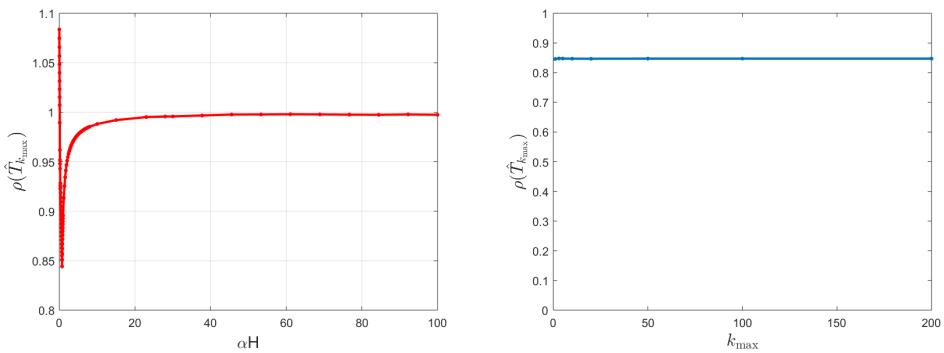

FIG. 4.3. *Spectral radius of* $\hat{T}_{k_{\max}}$*, for* $p, q = 10$*, with normalized overlap* $\bar{\gamma} = 0.01$*. Left:* $k_{\max} = 20$ *and normalized boundary parameter* $\bar{\alpha} \in [0.01, 100]$*. Right: Varying* $k_{\max}$*, with normalized boundary parameter* $\bar{\alpha} = 0.72$*.*

$\hat{T}_{k_{\max}}$ and the number of iterations to achieve convergence of the ORAS method, respectively, for different values of the normalized parameter $\bar{\alpha} = \alpha H$, for a 2×2 partition of the unit square, and $\bar{\gamma} = 0.05$. Note that the value of α corresponding to the smallest spectral radius of the truncated matrix coincides with the value of α producing the smallest number of iterations to achieve convergence of the ORAS method.

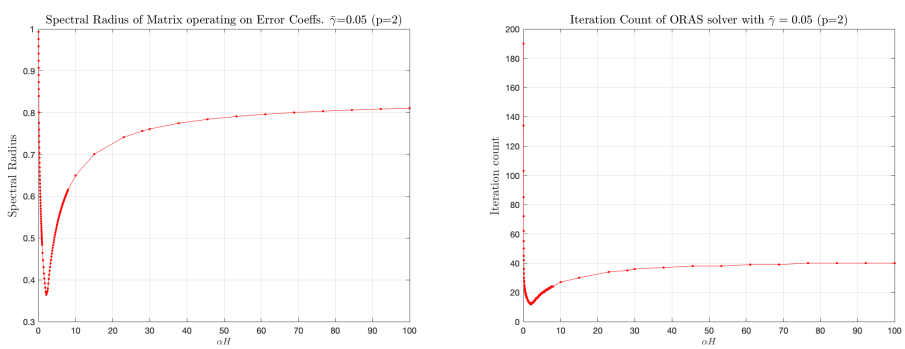

FIG. 4.4. *Left: Spectral radius of* $\hat{T}_{k_{\max}}$ *for* $k_{\max} = 13$*. Right: Number of iterations to converge (relative residual norm below* 10^{-6}*). In both cases, the plots are for different values of the normalized parameter* $\bar{\alpha} = \alpha H$*, for* $p = q = 2$*, and a normalized overlap* $\bar{\gamma} = 0.05$*.*

We end this section by remarking that, as we mentioned in the introduction, we believe that this is the first proof of convergence of an optimized Schwarz iteration for multiple subdomains in two dimensions with cross-points at the continuous level, except of course for the summarized treatment in our conference paper [22].

5. Asynchronous optimized Schwarz methods. We want to analyze the convergence of an asynchronous implementation of the OS iteration (2.2) for the interior subdomains and similar equations describing the method for the subdomains on the boundary of Ω. In other words, a processor would solve the local problem (2.2) with the boundary information received from the other processors, and when the solution is obtained, it is sent to the other processors. Then, without synchronizing with the other processors, the process is repeated using whatever information (if any) has been received by the other processors. There is a rich

literature on asynchronous methods beginning with the work of Chazan and Miranker [9], Baudet [5], Robert [36], Bertsekas [6], Lubachevsky and Mitra [27], Elsner, Koltracht, and Neumann [16], Bru, Migallón, and Penadés [8], El Baz, Gazen, Miellou, and Spiteri [12, 13], Barán, Kaszkurewicz, and Bhaya [4], Bahi [2], and El Tarazi [15], among others.

We begin by reviewing a mathematical model of asynchronous iterations. This is a standard model and can be found, e.g., in [7, 19, 38]. Let $U^{(1)}, \dots, U^{(R)}$ be given sets and U be their Cartesian product, i.e., $U = U^{(1)} \times \cdots \times U^{(R)}$. Thus, $u \in U$ implies $u = \left(u^1, \dots, u^R\right)$, with $u^\nu \in U^{(\nu)}$ for $\nu \in \{1, \dots, R\}$. Let $T^{(\nu)} : U \to U^{(\nu)}$, where $\nu \in \{1, \dots, R\}$, and let $T : U \to U$ be a vector-valued map (the iteration map) given by $T = (T^{(1)}, \dots, T^{(R)})$ with a fixed point u_*, i.e., $u_* = T(u_*)$. Let us define a *time stamp* as the instant of time at which at least one processor finishes its computation and produces a new update. Let $\{t_n\}_{n\in\mathbb{N}}$ be a sequence of time stamps at which at least one processor updates its associated component. Let $\{\sigma(n)\}_{n\in\mathbb{N}}$ be a sequence with $\sigma(n) \subset \{1, \dots, R\}$ for all $n \in \mathbb{N}$. The set $\sigma(n)$ consists of labels (numbers) of the processors that update their associated component at the nth time stamp. Define, for $\nu, \tilde{q} \in \{1, \dots, R\}$, $\{\tau_{\tilde{q}}^{\nu}(n)\}_{n\in\mathbb{N}}$ a sequence of integers representing the time-stamp index of the update of the data coming from processor $\tilde{q}$ and available in processor ν at the beginning of the computation of $u_n^{(\nu)}$ which ends at the time stamp t_n. Let $u_0 = \left(u_0^1, \dots, u_0^R\right)$ be the initial approximation (of the fixed point u_*). Then, the new computed value updated by processor ν at the nth time stamp is

$$u_n^\nu = \begin{cases} T^{(\nu)}\left(u^1_{\tau_1^\nu(n)}, \dots, u^R_{\tau_R^\nu(n)}\right), & \nu \in \sigma(n), \\ u_{n-1}^\nu, & \nu \notin \sigma(n). \end{cases} \tag{5.1}$$

In other words, at the time stamp t_n either u^ν is updated (if $\nu \in \sigma(n)$) or it is not (if $\nu \notin \sigma(n)$). It is assumed that the three following conditions (necessary for convergence) are satisfied:

$$\tau_{\tilde{q}}^{(\nu)}(n) < n, \qquad \forall \nu, \tilde{q} \in \{1, \dots, R\}, \forall n \in \mathbb{N}, \tag{5.2}$$

$$\operatorname{card}\{n \in \mathbb{N}^* | \nu \in \sigma(n)\} = +\infty, \qquad \forall \nu \in \{1, \dots, R\}, \tag{5.3}$$

$$\lim_{n\to+\infty} \tau_{\tilde{q}}^{(\nu)}(n) = +\infty, \qquad \forall \nu, \tilde{q} \in \{1, \dots, R\}. \tag{5.4}$$

Condition (5.2) indicates that data used at time t_n must have been produced before the beginning of the computation of $u_n^{(\nu)}$, i.e., time does not flow backward. Condition (5.3) means that no process will ever stop updating its components. Condition (5.4) corresponds to the fact that new data will always be provided to the process. In other words, no process will have a piece of data that is never updated.

The standard convergence results for the asynchronous iteration (5.1) that one uses for the analysis of asynchronous iterations are those in [7, 9, 15] (see also [19]). Here we state a theorem due to Bertsekas [7], extended to infinite products in [17] and further to operators which change from one iteration to the next in [18]. Our convergence proof of the asynchronous version of the OS method (2.2) will consist of showing that the hypotheses of this theorem hold.

THEOREM 5.1. *Let $U = U^{(1)} \times \cdots \times U^{(R)}$, $T^{(\nu)} : U \to U^{(\nu)}$, $\nu \in \{1, \dots, R\}$, and $T = (T^1, \dots, T^{(R)})$ with a fixed point u_*, i.e., $u_* = T(u_*)$. Consider an asynchronous iteration of the form (5.1), and assume that the conditions (5.2)–(5.4) hold. Assume further that we have a non-empty set E_* and a sequence of non-empty sets $E_n \subset U$, with $E_n = E_n^{(1)} \times \cdots \times E_n^{(R)}$ and $E_{n+1} \subseteq E_n$, $n = 0, 1, \dots$ If in addition,*

(i) $T(E_n) \subseteq E_{n+1} \subseteq E_n$ and

(ii) any limit point of any sequence $\{w_n\}_{n=0}^\infty$ with $w_n \in E_n$ lies in E_*.

Then, provided $u_0 \in E_0$, every limit point of the updates u_n of the asynchronous iteration (5.1) lies in E_*. In particular if $E_* = \{u_*\}$, then the asynchronous iteration (5.1) converges to u_*.

We are ready to finally define formally the asynchronous optimized Schwarz iterations. Let $l_1 = \tau^{(s,r)}_{(s-1,r)}(n)$, $l_2 = \tau^{(s,r)}_{(s+1,r)}(n)$, $l_3 = \tau^{(s,r)}_{(s,r-1)}(n)$, and $l_4 = \tau^{(s,r)}_{(s,r+1)}(n)$, i.e., the time-stamp indexes of the updates of the data coming from the neighboring processors and available in processor (s,r) at the beginning of the computation of $u^{(s,r)}_{t_n}$ which will end at the nth time stamp. Let us define the local equations for interior subdomains as

$$
\begin{cases}
-\Delta u^{(s,r)}_{t_n} = f^{(s,r)} & \text{in } \Omega^{(s,r)}, \\
-\dfrac{\partial u^{(s,r)}_{t_n}}{\partial x} + \alpha u^{(s,r)}_{t_n} = -\dfrac{\partial u^{(s-1,r)}_{t_{l_1}}}{\partial x} + \alpha u^{(s-1,r)}_{t_{l_1}} & \text{for } x = (s-1)h - \gamma, \\
\dfrac{\partial u^{(s,r)}_{t_n}}{\partial x} + \alpha u^{(s,r)}_{t_n} = \dfrac{\partial u^{(s+1,r)}_{t_{l_2}}}{\partial x} + \alpha u^{(s+1,r)}_{t_{l_2}} & \text{for } x = sh + \gamma, \\
-\dfrac{\partial u^{(s,r)}_{t_n}}{\partial y} + \alpha u^{(s,r)}_{t_n} = -\dfrac{\partial u^{(s,r-1)}_{t_{l_3}}}{\partial y} + \alpha u^{(s,r-1)}_{t_{l_3}} & \text{for } y = (r-1)h - \gamma, \\
\dfrac{\partial u^{(s,r)}_{t_n}}{\partial y} + \alpha u^{(s,r)}_{t_n} = \dfrac{\partial u^{(s,r+1)}_{t_{l_4}}}{\partial y} + \alpha u^{(s,r+1)}_{t_{l_4}} & \text{for } x = rh + \gamma.
\end{cases}
\tag{5.5}
$$

In our case, the processors are labeled with a pair of indices corresponding to the numbering of the subdomains, say (s,r). Analogously to the synchronous case, for the cases where the subdomains are not interior but touch a boundary, i.e., $s = 1$, $r = 1$, $s = p$, and/or $r = q$, the local equations are similar to (5.5) but have one or more Dirichlet homogeneous boundary conditions. The local approximation of the solution at time stamp t_n corresponding to the interior (s,r)-subdomain is

$$
u^{(s,r)}_{t_n} = \begin{cases} \text{solution of (5.5)}, & \text{if } (s,r) \in \sigma(n), \\ u^{(s,r)}_{t_{n-1}}, & \text{if } (s,r) \notin \sigma(n), \end{cases}
\tag{5.6}
$$

where $\sigma(n) \subset \{1,\dots,p\} \times \{1,\dots,q\}$. For subdomains touching the boundary we replace line one in equation (5.6) by the corresponding local equations.

Following the same process as in the synchronous case we can obtain local operators that relate the error coefficients at different time stamps. These local operators are the same as in the synchronous case. In the asynchronous case, the local operations are performed without synchronization, therefore the expression of the global operator is more complex than in the synchronous case. However, as it is shown in the next section, we can study the convergence of the asynchronous method by considering the spectral properties of the operator $|\hat{T}|$, where $\hat{T}$ is the global operator of the synchronous case, and the absolute value is understood componentwise.

6. Convergence proof of the asynchronous OS method. We begin by reviewing some concepts from the literature. An $n \times n$ matrix T is irreducible if for every pair of indices i, j, there exists a path (of length $k = k(i,j)$) in the graph of T joining the index i with the index j. For a nonnegative matrix T, this is equivalent to say that there is an integer k such that the (i,j)-entry of T^k is nonzero (i.e., positive). The latter concept extends naturally to infinite matrices, and more general to operators on Banach spaces; see, e.g., [26][3].

[3] For generalized concepts of irreducibility on Banach spaces, see also, e.g., [34].

For our convergence result we assume that $\hat{T}$ and thus $|\hat{T}|$ is irreducible (which it is in our case; see Figure 4.1). Since $|\hat{T}|$ is nonnegative and irreducible, it has a positive Perron eigenvector corresponding to the spectral radius, i.e., there exists $v > 0$ such that $|\hat{T}|v = \rho v$ with $\rho = \rho(|\hat{T}|)$; see, e.g, [26]. This eigenvector is of course unique up to scaling, and it has finite norm. This property is used in the proof of the theorem. As it will follow from the proof of the theorem, instead of requiring the infinite matrix to be irreducible and thus its absolute value having a positive Perron vector, it would suffice to assume that there exists a positive vector v (with finite norm) so that $|\hat{T}|v \leq \rho v$ for $\rho < 1$.

We show in Section 7, that for certain subdomain configurations there are values of the normalized boundary parameter $\bar{\alpha} = \alpha H$ and the normalized overlap $\bar{\gamma} = \gamma/H$ for which $\rho(|\hat{T}_{k_{\max}}|) < 1$, where H is the side length of the subdomains. Also, for these configurations the value of $\rho(|\hat{T}_{k_{\max}}|) < 1$ remains practically constant for large enough $k_{\max}$, which implies that $\rho(|\hat{T}|) < 1$. These observations allow us to consider $\rho(|\hat{T}|) < 1$ as a viable hypothesis to prove the convergence of the asynchronous OS (AOS) method for the given Poisson's problem at the continuous level.

THEOREM 6.1. *Let $\hat{T}$ be the operator which maps the coefficients of the series representing the error of the synchronous iteration* (2.2) *(and similarly for the subdomains touching the boundaries) at step n to those at step $n+1$, for example, as defined by* (C.16)*. Assume that $|\hat{T}|$ is irreducible, and let $v > 0$ be a corresponding Perron vector. Assume further that $\rho = \rho(|\hat{T}|) < 1$. Let $\mathbf{B}_1$ be the vector containing all the coefficients $B_{1,m,i}^{(s,r)}$ for the error after the first iteration in* (6.2)*, $i \in \{1, \ldots, 4\}$, $s \in \{1, \ldots, p\}$, and $r \in \{1, \ldots, q\}$. Recall that $\|\mathbf{B}_1\|_\infty$ is finite by Theorem 3.2. If there exists a positive constant $a > 0$ such that*

$$|\mathbf{B}_1| \leq av, \tag{6.1}$$

then the asynchronous implementation of the optimized Schwarz iteration (5.6) *converges to the solution of* (2.1) *for any initial u_0 piecewise C^3-function in Ω.*

Proof. Given the initial function approximation u_0, we consider the initial error $\eta_0 = u_0 - u_*$. After the first update, all local errors $\eta_1^{(s,r)}$ can be represented in terms of the four parts given by the series (3.14)–(3.17), (3.22)–(3.29), which for each subdomain indexed by (s, r), $s = 1, \ldots, p$, $r = 1, \ldots, q$, we can write generically as in (3.30), i.e.,

$$\eta_1^{(s,r)}(x_\ell, y_\ell) = \sum_{i=1}^{4} \sum_{m=1}^{\infty} B_{1,m,i}^{(s,r)} \varphi_{m,i}^{(s,r)}(x_\ell, y_\ell). \tag{6.2}$$

Collecting all the coefficients of these series we have the infinite vector $\mathbf{B}_1$.

Let $w = av$. Then we have

$$|\hat{T}w| = |\hat{T}(av)| = a|\hat{T}v| \leq a|\hat{T}|v \leq a\rho v = \rho(av) = \rho w.$$

Thus,

$$|\hat{T}w| \leq \rho w. \tag{6.3}$$

Note that we also have

$$\|w\|_\infty = \|av\|_\infty = a\|v\|_\infty < \infty$$

since $\|v\|_\infty < \infty$ and $a < \infty$.

Let us define the set of functions $\bar{v}^{(s,r)} : \Omega^{(s,r)} \to \mathbb{R}$, defined on the (s, r)-subdomain by

$$E_n^{(s,r)} = \left\{ \bar{v}^{(s,r)} \;\middle|\; \bar{v}^{(s,r)} - u_*^{(s,r)} = \sum_{i=1}^{4} \sum_{m=1}^{\infty} B_{m,i}^{(s,r)} \varphi_{m,i}^{(s,r)} \text{ with } |\mathbf{B}^{(s,r)}| \leq \rho^{n-1} w^{(s,r)} \right\},$$

where $\mathbf{B}^{(s,r)}$ is the vector whose entries are the coefficients $B_{m,i}^{(s,r)}$. Define further the product set

$$E_n = E_n^{(1,1)} \times \cdots \times E_n^{(p,q)}.$$

It follows directly from these definitions that $E_{n+1} \subset E_n$, for $n = 1, 2, \ldots$ From (6.1) it also follows that $u_1 \in E_1$. We will show next that the conditions (i) and (ii) of Theorem 5.1 hold. Let $u \in E_n$, that is,

$$u^{(s,r)} - u_*^{(s,r)} = \sum_{i=1}^{4} \sum_{m=1}^{\infty} B_{m,i}^{(s,r)} \varphi_{m,i}^{(s,r)}, \qquad \text{with} \quad |\mathbf{B}^{(s,r)}| \leq \rho^{n-1} w^{(s,r)}, \tag{6.4}$$

and consider $T(u) = (T^{(1,1)}(u), \ldots, T^{(p,q)}(u))$, where $T^{(s,r)}(u)$ is the solution of the problem (5.5) (or the corresponding equations for subdomains touching the boundary). By Theorem 3.2, we can write

$$T^{(s,r)}(u) - u_*^{(s,r)} = \sum_{i=1}^{4} \sum_{m=1}^{\infty} C_{m,i}^{(s,r)} \varphi_{m,i}^{(s,r)}. \tag{6.5}$$

In other words, we have

$$\mathbf{C}^{(s,r)} = \hat{T}^{(s,r)} \mathbf{B},$$

where we have collected all the entries of the coefficients $B_{m,i}^{(s,r)}$ into the vector $\mathbf{B}$, $m = 1, 2, \ldots, i \in \{1, \ldots, 4\}$, $s \in \{1, \ldots, p\}$, and $r \in \{1, \ldots, q\}$, and all the entries of $\mathbf{C}_{m,i}^{(s,r)}$ into the vector $\mathbf{C}^{(s,r)}$, $m = 1, 2, \ldots, i \in \{1, \ldots, 4\}$. We need to show the bound $|\mathbf{C}^{(s,r)}| \leq \rho^{(n+1)-1} w^{(s,r)}$. Note that from (6.4) it follows that $|\mathbf{B}^{(s,r)}| \leq \rho^{n-1} w^{(s,r)}$, for all $s \in \{1, \ldots, p\}$ and $r \in \{1, \ldots, q\}$. Hence,

$$|\mathbf{B}| \leq \rho^{n-1} w\,.$$

Then, using (6.3) we have

$$\begin{aligned} |\mathbf{C}^{(s,r)}| &= |\hat{T}^{(s,r)} \mathbf{B}| \leq |\hat{T}^{(s,r)}||\mathbf{B}| \leq |\hat{T}^{(s,r)}| \rho^{n-1} w = \rho^{n-1} \left(|\hat{T}^{(s,r)}| w \right) \\ &\leq \rho^{n-1} \rho w^{(s,r)} = \rho^{(n+1)-1} w^{(s,r)}. \end{aligned} \tag{6.6}$$

Given that (s, r) was arbitrary, we have that this inequality holds for all $s \in \{1, \ldots, p\}$, $r \in \{1, \ldots, q\}$. Then, by (6.5) and (6.6), $T^{(s,r)}(u) \in E_{n+1}^{(s,r)}$ for all $s \in \{1, \ldots, p\}$ and $r = \{1, \ldots, q\}$. Consequently, $T(u) = (T^{(1,1)}(u), \ldots, T^{(p,q)}(u)) \in E_{n+1}$. Since $u \in E_n$ was arbitrary, we have $T(u) \in E_{n+1}$ for all $u \in E_n$. Therefore,

$$T(E_n) \subset E_{n+1} \subset E_n.$$

Thus, condition (i) of Theorem 5.1 holds.

We show now that condition (ii) of Theorem 5.1 holds. Using Lemma G.1 in Appendix G, we have that each local error $\eta_n^{(s,r)} = T^{(s,r)}(u) - u_*^{(s,r)}$ is bounded as follows:

$$|\eta_n^{(s,r)}(x_\ell, y_\ell)| \leq 4 \|\mathbf{B}_n\|_\infty M S,$$

where M is a positive constant independent of n and

$$S = \max \left\{ \sum_{m=1}^{\infty} \frac{1}{z_m^{5/2}}, \sum_{m=1}^{\infty} \frac{1}{\tilde{z}_m^{5/2}} \right\}.$$

Then, since $\|\mathbf{B}_n\|_\infty \leq \rho^{n-1}\|w\|_\infty$, we have the bound

$$|\eta_n^{(s,r)}(x_\ell, y_\ell)| \leq 4\rho^{n-1}\|w\|_\infty MS. \tag{6.7}$$

Then, since $\rho < 1$ and $\|w\|_\infty < \infty$, we have

$$\lim_{n\to\infty} |\eta_n^{(s,r)}(x_\ell, y_\ell)| = 0$$

uniformly in $(x_\ell, y_\ell) \in \Omega^{(s,r)}$, which implies that for all $u_1 \in E_1$ we have

$$\lim_{n\to\infty} \|T^n(u_1)\|_\infty = u_*.$$

Thus, condition (ii) of Theorem 5.1 holds.

Therefore, the asynchronous optimized Schwarz method converges. ∎

7. Spectral radius of $\hat{T}_{k_{\max}}$ and $|\hat{T}_{k_{\max}}|$. Recall that $\hat{T}_{k_{\max}}$ is a finite matrix obtained by discarding the rows and columns of $\hat{T}$ corresponding to the coefficients pertaining to $k > k_{\max}$. Recall also that we are considering a domain consisting of $p \times q$ (overlapping) rectangular subdomains. The values of the entries of the matrix $\hat{T}_{k_{\max}}$ depend on $\bar{\gamma}$, $\bar{\alpha}$ (the normalized overlap and normalized $OO0$ parameter), and $k_{\max}$. The structure of the matrix depends on $k_{\max}$, p, q, and the way we order the entries of the infinite vector $\mathbf{B}_n$, i.e., the way we order each coefficient $B_{n,k,i}^{(s,r)}$ based on the values of s, r, k, and i. However, the eigenvalues (and thus the spectral radius) do not depend on the ordering of the entries since a change in the order is just a similarity transformation obtained through permutation matrices. For the ordering that we have chosen (as described at the end of Section 3), we computed the spectral radius of the resulting matrix $\hat{T}_{k_{\max}}$, for $\bar{\gamma} \in \{0, 0.01, 1/30, 0.04, 0.1, 0.13, 0.18, 0.2, 0.25\}$, a set of values of $\bar{\alpha}$ in the range $[0.01, 500]$, $k_{\max} \in \{1, 2, 3, 5, 10, 20, 50, 100, 200, 400\}$, and $p, q \in \{5, 10, 20, 30, 40\}$. In these computations we have observed the following.

1. There exist values of $\bar{\alpha}$ for which the spectral radius of $\hat{T}_{k_{\max}}$ is less than one.
2. For a given $\bar{\gamma}$ and the range of $\bar{\alpha}$ considered in the experiments, $\rho(\hat{T}_{k_{\max}})$ has a minimum, and it approaches a constant less than one for large values of $\bar{\alpha}$; see Figure 4.3, left.
3. Given $\bar{\gamma}$, $\bar{\alpha}$, p, and q, the value of $\rho(\hat{T}_{k_{\max}})$ remains practically constant for large enough $k_{\max}$; see Figure 4.3, right.
4. For a given $\bar{\gamma}$, the optimal spectral radius of $\hat{T}_{k_{\max}}$ increases as the number of subdomains $p \times q$ increases; see Figure 7.1, left.
5. The optimal spectral radius of $\hat{T}_{k_{\max}}$ decreases as $\bar{\gamma}$ increases up to a certain point; see Figure 7.1, right.

In Figure 7.2, left, a plot of the values of the spectral radius of $|\hat{T}_{k_{\max}}|$ for different values of $\bar{\alpha}$ is shown for the case $\bar{\gamma} = 0.01$, $p, q = 2$, and $k_{\max} = 100$. From (C.9) we know that

$$|B_{m,1,i}^{(s,r)}| \leq \frac{C_1}{z_m^{1/2}}$$

for some $C_1 > 0$. Similarly, for subdomains touching the boundary like in a partition with $p = q = 2$, we have

$$|B_{m,1,i}^{(s,r)}| \leq \frac{C_1}{\tilde{z}_m^{1/2}}$$

for some $C_1 > 0$, where without loss of generality we have used the same constant in both cases. In Figure 7.2, right, we see the plot of the entries of the Perron vector of $|\hat{T}_{k_{\max}}|$ for

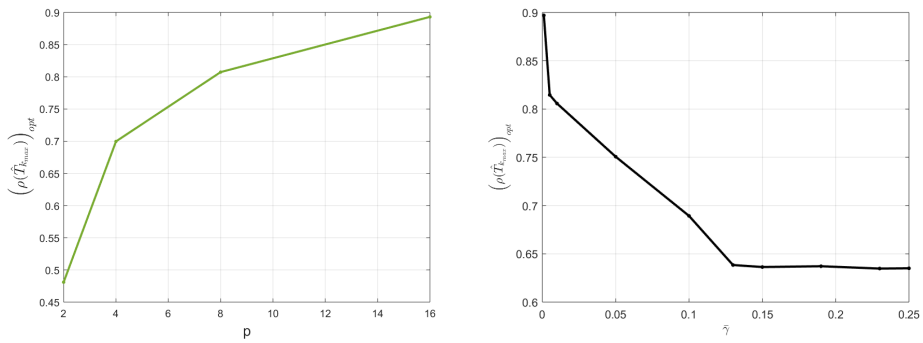

FIG. 7.1. *Optimal spectral radius of* $\hat{T}_{k_{\max}}$. *Left: For varying* p, *for* $\bar{\gamma} = \frac{\gamma}{H} = 0.01$, *and* $k_{\max} = 7$, *where the number of subdomains is* $p \times q = p^2$ *(i.e.,* $q = p$*). Right: For varying normalized overlap* $\bar{\gamma} = \frac{\gamma}{H}$, *for* $p, q = 8$, *and* $k_{\max} = 10$.

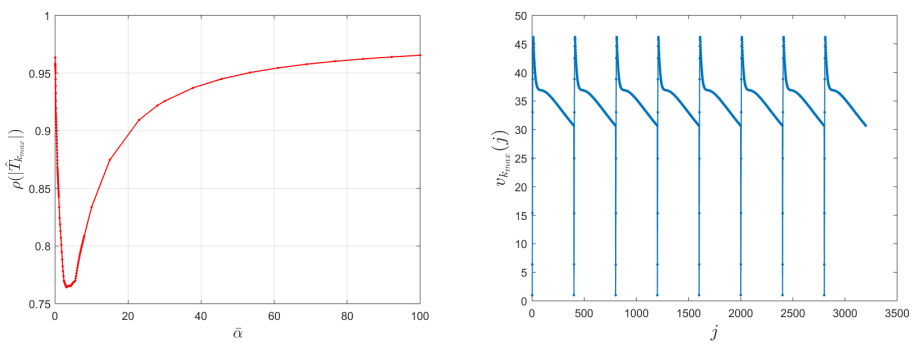

FIG. 7.2. *Left: Spectral radius of* $|\hat{T}_{k_{\max}}|$ *for varying* $\bar{\alpha}$, *for* $p, q = 2$, *and* $\bar{\gamma} = 0.01$. *Right: Entries of the Perron vector of* $|\hat{T}_{k_{\max}}|$, *for* $\bar{\alpha} = 2.54$, $\bar{\gamma} = 0.01$, *and* $k_{\max} = 400$.

$\bar{\alpha} = 2.54, \bar{\gamma} = 0.01, p, q = 2$. This plot is formed by the repetition of the part of the graph that goes from $j = 1$ to $j = k_{\max}$. In Figure 7.3 we have the log-log plot of this part of the Perron vector. From this plot we see that for all $s \in \{1, \dots, p\}, r \in \{1, \dots, q\}, i \in \{1, \dots, 4\}$, we have $v^{s,r}_{1,i,k_{\max}} = 1$ and

$$v^{(s,r)}_{m,i,k_{\max}} > \frac{1}{(m-1)^{1/2}} \tag{7.1}$$

for $m \in \mathbb{N} \setminus \{1\}$. In fact (7.1) holds for all $k_{\max}$. Then,

$$v^{(s,r)}_{m,i} \geq \frac{1}{(m-1)^{1/2}},$$

for $m \in \mathbb{N} \setminus \{1\}$ and $v^{s,r}_{1,i} = 1$.

Let $C_2 = \max\left\{1, \frac{1}{\tilde{z}_1^{1/2}}\right\}$. For $m > 1$ we have

$$v^{(s,r)}_{m,i} \geq \frac{1}{(m-1)^{1/2}} > \frac{1}{((m-1)\pi)^{1/2}} > \frac{1}{\tilde{z}_m^{1/2}} \tag{7.2}$$

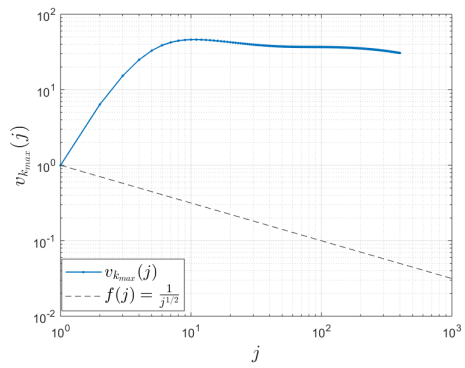

FIG. 7.3. *Log-log plot of part of the Perron vector of* $|\hat{T}_{k_{\max}}|$, *for* $j \in [1, k_{\max}]$, $\bar{\alpha} = 2.54$, $\bar{\gamma} = 0.01$, *and* $k_{max} = 400$.

since $(m-1)\pi \leq \tilde{z}_m \leq m\pi$. Then, from (7.2) and since $C_2 \geq 1$ we have for $m > 1$,

$$C_2 v_{m,i}^{(s,r)} > \frac{1}{\tilde{z}_m^{1/2}}.$$

Also, since $v_{1,i}^{(s,r)} = 1$, we have

$$C_2 v_{1,i}^{(s,r)} = C_2 = \max\left\{1, \frac{1}{\tilde{z}_1^{1/2}}\right\}.$$

Consequently,

$$C_2 v_{m,i}^{(s,r)} \geq \frac{1}{\tilde{z}_m^{1/2}}$$

for all $m \in \mathbb{N}$. Then, taking $a = C_1 C_2$, and since $B_{m,1,i}^{(s,r)} \leq C_1/\tilde{z}_m^{1/2}$, we have $av \geq |\mathbf{B}_1|$. Additionally, we have that $\rho(|\hat{T}_{k_{\max}}|) < 0.8$ for all $k_{\max} \in \mathbb{N}$. Thus, the conditions of Theorem 6.1 hold, and the convergence of the asynchronous implementation of OS is guaranteed for $\bar{\alpha} = 2.54$, $\bar{\gamma} = 0.01$, $p, q = 2$.

We remark that the discussion we just presented for $p = q = 2$ does not carry over to larger values of p, q for the asynchronous case. This situation arises because (6.7) is not a tight upper bound for the asymptotic convergence of the method. Nevertheless, as we see in Section 9, convergence is achieved in the asynchronous case for larger values of p, q.

8. Optimal Robin parameter α. For large enough $k_{\max}$ such that $\rho(\hat{T}_{k_{\max}}) < 1$, the spectral radius of $\hat{T}_{k_{\max}}$ describes the asymptotic convergence rate of the optimized Schwarz method for the synchronous case. Thus, in the synchronous case we define the optimal $\bar{\alpha}$ for a given (normalized) overlap amount $\bar{\gamma}$ as the one which minimizes the spectral radius of $\hat{T}_{k_{\max}}$ and thus gives the optimal asymptotic convergence rate. Note that $\hat{T}_{k_{\max}}$ is a banded square matrix of order $N = 2k_{\max}(2pq - p - q)$. Let $\rho_\infty = \lim_{k_{\max}\to\infty} \rho(\hat{T}_{k_{\max}})$. Usually, for $k_{\max} = 5$ we have that $\rho(\hat{T}_{k_{\max}})$ is a good estimation of ρ_∞ when p and q are large. Thus, *computing the spectral radius of* $\hat{T}_{k_{\max}}$ *is not an expensive operation.* Consequently, finding the optimal $\bar{\alpha}$ is not an expensive operation.

The spectral radius of $\hat{T}_{k_{\max}}$ is a function of the normalized Robin parameter $\bar{\alpha}$, the normalized overlap $\bar{\gamma}$, the number of subdomains in each direction p and q, and the truncation

parameter $k_{\max}$. The optimal value of $\bar{\alpha}$ is a function of $\bar{\gamma}$, p, q. In Figure 8.1, left, we see the optimal values of $\bar{\alpha}$ for $\bar{\gamma} \in [0.0005, 0.06]$ and $p = q$ with $p \in \{4, 5, 6, 8\}$. As it can be observed, the range of values of $\bar{\gamma}$ for which the values of $\bar{\alpha}_{opt}$ are essentially constant increases with p. Thus, for large p we have that $\bar{\alpha}_{opt}$ is constant for all $\bar{\gamma} \in [0.0005, 0.06]$ (i.e., for an overlap between 0.1% and 12%), and it only depends on the number of subdomains, i.e., it only depends on the parameter p. In Figure 8.1, right, we see the values of $\bar{\alpha}_{opt}$ for $p \in [4, 40] \cap \mathbb{N}$ using $\bar{\gamma} = 0.01$. The red curve is an approximation of the blue curve by using the following power law formula,

$$\bar{\alpha}_{opt} = 8.9p^{(-1.08)}. \tag{8.1}$$

Thus, for $p \in [10, 40] \cap \mathbb{N}$ we can use (8.1) to obtain the optimal value of $\bar{\alpha}$.

In the computation of the optimal $\bar{\alpha}$ we have taken $k_{\max}$ large enough (i.e., $k_{\max} = 40$) so that $\rho\left(\hat{T}_{k_{\max}}\right)$ remained essentially constant for larger values of $k_{\max}$. With this we ensure that the computed value of $\bar{\alpha}_{opt}$ is essentially the same as the value of $\bar{\alpha}_{opt}$ corresponding to the infinite-dimensional case.

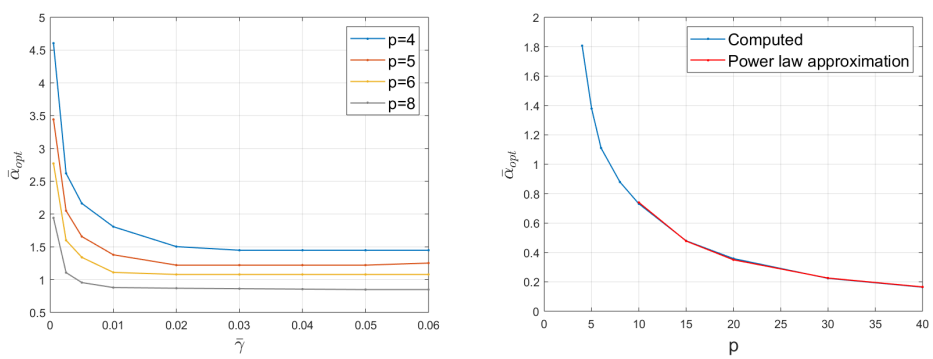

FIG. 8.1. *Left: Optimal values of $\bar{\alpha}$ for different values of $\bar{\gamma}$ and p. Right: Computed values of $\bar{\alpha}_{opt}$ for different values of p and the power law approximation for large values of p and for $\bar{\gamma} = 0.01$.*

9. Numerical experiments. We present numerical experiments that illustrate the performance of the proposed asynchronous optimized Schwarz method on a bounded domain as well as the synchronous counterpart. The experiments show the convergence of the methods, illustrating the results of our theorems. In addition it can be observed that the asynchronous version is faster in terms of execution time.

The test cases are related to the study of the heat analysis in a domain, modeled as follows:

$$\rho \frac{\partial u}{\partial t} - \nabla \cdot (k \nabla u) = f,$$

where u denotes the thermal field, k is the thermal conductivity, and f the heat-flux density of the source. Here the steady-state heat equation is considered, i.e.,

$$\frac{\partial u}{\partial t} = 0,$$

which is by definition not time-dependent and which corresponds to the case where enough time has passed such that the thermal field no longer evolves in time. This leads to the

following reduced equation

$$-k\Delta u = f.$$

Two numerical experiments are conducted: the first one on a two-dimensional domain and the second one on a three-dimensional domain.

Car compartment. The numerical solution of the steady-state heat equation required for the first study was performed on a two-dimensional domain of dimensions 1760 mm $\times$ 745 mm representing a cross section of a car compartment. This area is meshed with unstructured quadrangle finite elements. One example of the finite element mesh with 465 degrees of freedom (DOF) is shown Figure 9.1, left. We considered for the simulation a

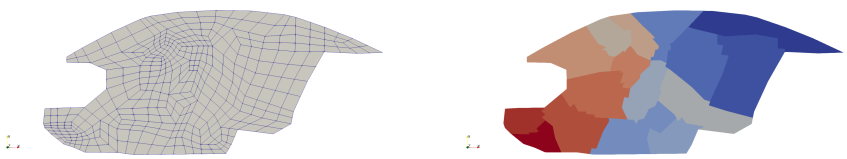

FIG. 9.1. *Left: Finite element mesh of a two-dimensional cross section of the car compartment. Right: Its partitioning into subdomains.*

refinement of the mesh which contain 46 945 DOF. Lagrange Q_1 finite elements are used for the discretization. The domain is split into subdomains, and one example of the partitioning into 16 subdomains with the METIS software [25] is shown in Figure 9.1, right.

We consider three different situations, namely a partitioning of the domain into 16, 25, and 36 subdomains. In all cases, the overlap used is the minimum overlap, i.e., one set of common nodes in the boundary between subdomains. The optimized coefficients of the Schwarz algorithms are obtained using the values of $\rho(\hat{T}_{k_{\max}})$ and $\rho(|\hat{T}_{k_{\max}}|)$ in terms of $\bar{\alpha} = \alpha H$ (see, e.g., Figures 4.3 (left) and 7.2 (left)), with the minimum found using the CMA-ES algorithm from [29]. Here H is the diameter of the subdomains. The resulting parameters where divided by H, leading to (non-normalized) values of the synchronous optimized parameter α equal to 0.0039068×10^3, 0.0038607×10^3, 0.0034090×10^3 for a partitioning into 16, 25, and 36 subdomains, respectively. The same value of the parameters are used for the synchronous and asynchronous version of the code.

To solve the resulting linear system, the synchronous and asynchronous optimized Schwarz methods with zeroth-order optimized interface conditions were implemented in the C++ library *Alinea* [28]. The parallel implementation of the asynchronous optimized Schwarz methods is quite similar to the synchronous implementation described in [32] except that the asynchronous iterations and asynchronous communications are managed by a new additional layer. This new additional layer, the C++ library *JACK* [30], is defined on top of the MPI library; the version of the MPI library used in the experiments is MPICH2 [1]. This layer allows us to use asynchronous communications between the processors and to deal with continuous requests. This new layer also contains new functionality such as the detection of the asynchronous convergence of the algorithm for a given stopping criteria. Here we use the stopping criterion developed in [3]; it is based on a leader election protocol over a tree topology, where cancellation messages are introduced in order to avoid erroneous detections [31].

The experiments are performed on a heterogeneous cluster composed of four nodes Intel(R) Xeon(R) E5410, 2,33GHz, 8 cores, RAM: 8 GB, four nodes Intel(R) Core(TM) i7 2,80GHz, 8 cores, RAM: 8 GB each with graphics processing units accelerator (Tesla

FIG. 9.2. *Computer aided design model of the City of Lyon.*

K20c 4799MB, GTX 570 1279MB), and four nodes Intel(R) Xeon(R) E5-2609, 2,10GHz, 24 cores, RAM: 16 GB each with graphics processing units accelerator (three of them with Quadro K4000 3071MB and one with Quadro K600 1023MB), for a total of 160 cores. The interconnected network is a switched, star shaped 10Mb/s Ethernet network. We report our computational results in Table 9.1, where we vary the number of subdomains using the same discretization.

TABLE 9.1
Number of iterations or average and maximum updates and computational time (in seconds).

#subdomains	# iter	time	# updates avg	max	time
	Synchronous		Asynchronous		
16	109	2.79	151	224	1.73
25	187	2.42	261	497	1.10
36	304	1.76	332	705	0.75

Recall that in asynchronous iterations we cannot talk about (global) iteration steps since each processor may update its approximation to the (local) solution at different moments, i.e., at different time stamps. In fact, each processor (corresponding to each subdomain) would usually perform a different number of updates, i.e., of local solutions. Thus, in Table 9.1, for the synchronous case, the number of iterations are reported, while for the asynchronous case, the average and the maximum number of updates among all processors are reported. In both cases, the total computational time (in seconds) are shown. It can be appreciated that the asynchronous optimized Schwarz method performs better in terms of execution time than its synchronous counterpart. In fact, for each case, the time to converge for the asynchronous runs is about half the time needed in the synchronous case.

City of Lyon. In order to show the potential of the introduced approach, we present now some numerical experiments on a three-dimensional domain. The problem consists of a climate change modeling of the Rhône-Alps area, located in the southeast of France. The eastern part of the region is composed of the *Alps* mountain range. The western part of the region is composed of the start of the *Massif Central* mountain range. The central part of the region comprises the valleys of the Rhône and the Saône rivers. The City of Lyon Global Positioning System coordinates location are a latitude of 45.764043 degrees north and a longitude of 4.835659 degrees. The wind blows often in the Rhône-Alps area: the north wind is felt regularly from the north of the Rhône valley and the south wind blows sometimes

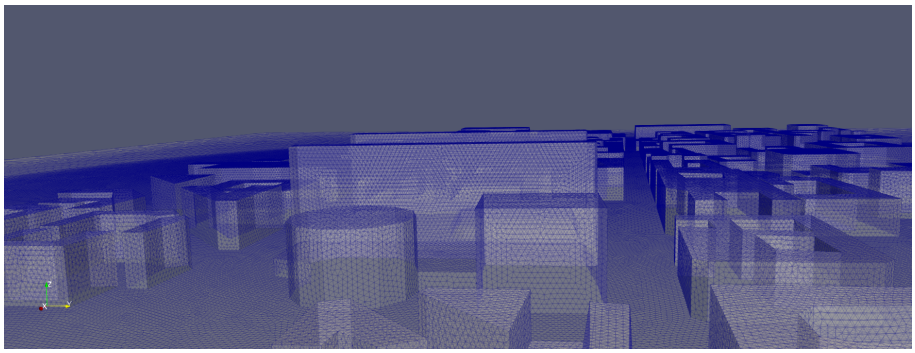

FIG. 9.3. *Finite element mesh of a three-dimensional model of the City of Lyon. Close up around some buildings.*

violently ahead of the disturbances from the Mediterranean and the southwest. This wind regime is the result of the alignment of the Rhône-Saône valleys and the ridges to the west (Massif Central) and to the east (Alps), which channel the wind in the valley. In addition to violent winds, polar cold wave and heat wave transported by the wind become a major interest.

We have realized a computer aided design model of the City of Lyon of dimensions 1600000 mm $\times$ 1600000 mm $\times$ 200000 mm, as shown in Figure 9.2. A focus on the area surrounding the Lyon train station is of particular attention during a heat wave, due to the presence of high buildings and the absence of gardens and parks. The finite element mesh is composed of 887 397 points. An example of the finite element mesh of a part of the boundary is shown in Figure 9.3. Lagrange P_1 finite elements are used for the discretization. The domain is split into subdomains, and one example of the partitioning into 16 subdomains with the METIS software [25] is shown Figure 9.4.

The optimized coefficients are derived from our two-dimensional theorems, with a minimum overlap, leading to $\bar{\alpha}$ equal to 0.0017119×10^3, 0.0012373×10^3, 0.0011186×10^3 for a partitioning into 16, 25, and 36 subdomains respectively. An example of the heat distribution is illustrated in Figure 9.5.

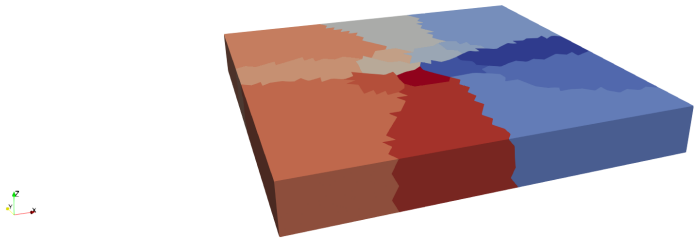

FIG. 9.4. *Mesh partitioning of the finite element mesh of a three-dimensional model of the City of Lyon.*

As shown in Table 9.2, the asynchronous optimized Schwarz method performs better in CPU time than its synchronous counterpart, despite requiring more iterations, confirming the efficiency of the proposed asynchronous approach. Indeed, for the cases of 25 and 36

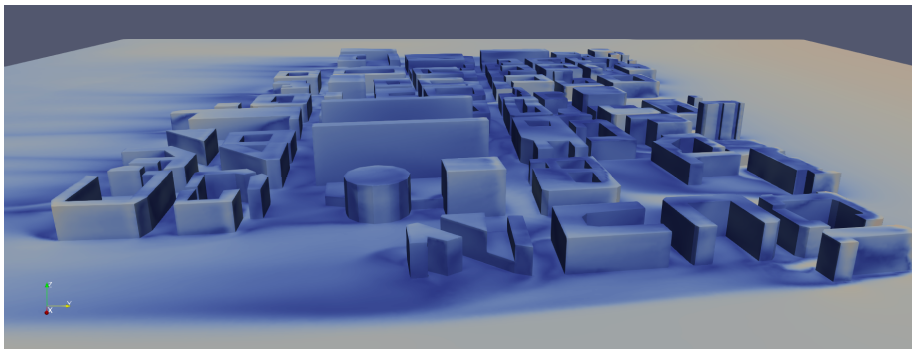

FIG. 9.5. *Heat distribution within a three-dimensional model of the City of Lyon.*

TABLE 9.2
Number of iterations or average and maximum updates and computational time (in seconds).

#subdomains	# iter	time	# updates avg	max	time
	Synchronous		Asynchronous		
16	825	73.8	951	1176	59.9
25	985	58.2	1223	1691	28.7
36	1474	34.8	1547	2762	14.3

subdomains, the asynchronous method takes less than half the computational time than the synchronous counterpart.

10. Conclusion. We have analyzed at the continuous level the convergence of the optimized Schwarz method when it is applied as an outer solver for the solution of Poisson's problem in a rectangular domain with Dirichlet (physical) boundary conditions and Robin artificial boundary conditions. We presented convergence proofs for the synchronous and asynchronous implementations of the optimized Schwarz method. As a key preliminary step to prove convergence we recasted the problem into a fixed point iteration with an infinite matrix as the iteration operator $\hat{T}$. Then we showed that to prove convergence of the method in the synchronous case, it suffices to study the spectral properties of a truncated version of this operator $\hat{T}_{k_{\max}}$, a finite matrix. This matrix is of very small dimension, and examining the eigenvalues of this matrix is computationally very inexpensive. In other words, with our proof we have reduced the proof of convergence to a small computational step. For the convergence proof of the asynchronous case, it suffices to study the spectral properties of $|\hat{T}_{k_{\max}}|$. We defined the optimal values of the Robin parameter as those whose normalized values minimize the spectral radius of $\hat{T}_{k_{\max}}$ for the synchronous case and that of $|\hat{T}_{k_{\max}}|$ for the asynchronous case. Finally, we presented numerical experiments from practical applications illustrating that on the one hand the method indeed converges as the theory indicates and on the other hand that the asynchronous implementation is faster than its synchronous counterpart in terms of execution time.

Acknowledgements. We thank an anonymous referee who had found an error in an earlier version of this paper. We thank both referees for their questions, comments, and references, which helped to greatly enhance our presentation.

Appendix A. Proof of Lemma 3.1.

Proof of Lemma 3.1. Note first that

$$\frac{d}{dx_\ell}\left(\phi_m(x_\ell)\right) = \frac{d\phi_m}{dx_\ell}(x_\ell)\frac{dx_\ell}{dx} = \frac{d\phi_m}{dx_\ell}(x_\ell)$$

since from the definition (3.1), $\frac{dx_\ell}{dx} = 1$. Similarly,

$$\frac{d}{dy}\left(\psi_m(H-y_\ell)\right) = \frac{d}{dy_\ell}\left(\psi_m(H-y_\ell)\right) = -\frac{d\psi_m}{dy_\ell}(H-y_\ell).$$

Then, it follows that

$$\frac{d^2\phi_m}{dx^2}(x_\ell) = \frac{d^2\phi_m}{dx_\ell^2}(x_\ell) \quad \text{and} \quad \frac{d^2}{dy^2}\left(\phi_m(H-y_\ell)\right) = \frac{d^2\phi_m}{dy_\ell^2}(H-y_\ell).$$

Also, note from the first line of equations (3.6) and (3.7) that

$$\frac{d^2\phi_m}{{dx_\ell}^2}(x_\ell) = -\left(\frac{z_m}{H}\right)^2\phi_m(x_\ell) \quad \text{and} \quad \frac{d^2\psi_m}{{dy_\ell}^2}(H-y_\ell) = \left(\frac{z_m}{H}\right)^2\psi_m(H-y_\ell).$$

Then, we have

$$\begin{aligned}\Delta(v_m(x_\ell,y_\ell)) &= \Delta(\phi_m(x_\ell)\psi_m(H-y_\ell))\\ &= \psi_m(H-y_\ell)\frac{d^2\phi_m}{{dx_\ell}^2}(x_\ell) + \phi_m(x_\ell)\frac{d^2\psi_m}{{dy_\ell}^2}(H-y_\ell)\\ &= -\psi_m(H-y_\ell)\left(\frac{z_m}{H}\right)^2\phi_m(x_\ell) + \phi_m(x_\ell)\left(\frac{z_m}{H}\right)^2\psi_m(H-y_\ell) = 0. \qquad \square\end{aligned}$$

Appendix B. Justification of the order interchange between derivatives, integral, and infinite summation.

LEMMA B.1. *The series in (3.14)–(3.17) with coefficients* $|B^{(s,r)}_{n,m,i}| \le M^{(s,r)}_n$ *with* $M^{(s,r)}_n > 0$ *are such that:*

1. *The order of the first derivatives and summation can be interchanged in* $[0,H]^2$.
2. *The order of the second derivatives and summation can be interchanged in* $(0,H)^2$.
3. *The order of the integral over* $[0,H]$*, the first derivatives, and summation can be interchanged.*

Proof. We present the proof for the case $i=1$, but a similar procedure can be used for the proof in the cases $i=2,3,4$.

Using (3.9), we have that

$$\eta^{(s,r)}_{n,1}(x_\ell,y_\ell) = \sum_{m=1}^{\infty}\frac{B^{(s,r)}_{n,m,1}}{z_m^{5/2}\left[\frac{\bar{\alpha}}{z_m}\sinh(z_m)+\cosh(z_m)\right]}\phi_m(x_\ell)\psi_m(H-y_\ell).$$

Let $\sigma=(\sigma_1,\sigma_2)$ be a multi-index. Then, we have $\partial^\sigma = \frac{\partial^{\sigma_1}}{\partial x_\ell}\frac{\partial^{\sigma_2}}{\partial y_\ell}$. Note that

$$\partial^\sigma\sum_{m=1}^{\infty}\frac{B^{(s,r)}_{n,m,1}}{z_m^{5/2}\psi_m(H)}\phi_m(x_\ell)\psi_m(H-y_\ell) = \sum_{m=1}^{\infty}\partial^\sigma\left(\frac{B^{(s,r)}_{n,m,1}}{z_m^{5/2}\psi_m(H)}\phi_m(x_\ell)\psi_m(H-y_\ell)\right)$$

for each $(x_\ell, y_\ell) \in (0,H)^2$ if the series on the right-hand side of the above equation converges uniformly in a neighborhood of each (x_ℓ, y_ℓ). Thus, in order to prove parts 1 and 2 of the lemma, it suffices to show that

$$\sum_{m=1}^{\infty} \partial^\sigma \left(\frac{B_{n,m,1}^{(s,r)}}{z_m^{5/2}\psi_m(H)} \phi_m(x_\ell)\psi_m(H-y_\ell) \right) \tag{B.1}$$

converges uniformly for $\sigma = (0,1)$, $\sigma = (1,0)$ in $[0,H]^2$ and for $\sigma = (0,2)$, $\sigma = (2,0)$ in $(0,H)^2$.

We have that

$$\sum_{m=1}^{\infty} \frac{\partial}{\partial y_\ell} \left(\frac{B_{n,m,1}^{(s,r)}}{z_m^{5/2}\psi_m(H)} \phi_m(x_\ell)\psi_m(H-y_\ell) \right) = \sum_{m=1}^{\infty} \frac{B_{n,m,1}^{(s,r)}}{z_m^{5/2}\psi_m(H)} \phi_m(x_\ell) \frac{\partial}{\partial y_\ell} \left(\psi_m(H-y_\ell)\right).$$

Note that $|\phi_m(x_\ell)| \le \bar{\alpha}/z_1 + 1$ in $[0,H]$ and

$$\frac{\frac{\partial}{\partial y_\ell}\left(\psi_m(H-y_\ell)\right)}{z_m\psi_m(H)} = \frac{\frac{-\bar{\alpha}}{H}\cosh\left(\frac{(H-y_\ell)z_m}{H}\right) - \frac{z_m}{H}\sinh\left(\frac{(H-y_\ell)z_m}{H}\right)}{z_m\left[\frac{\bar{\alpha}}{z_m}\sinh(z_m) + \cosh(z_m)\right]}$$
$$= \frac{1}{H}\frac{\frac{-\bar{\alpha}}{z_m} - \tanh\left(\frac{(H-y_\ell)z_m}{H}\right)}{\frac{\bar{\alpha}}{z_m}\tanh(z_m)+1}\left(\frac{\cosh\left(\frac{(H-y_\ell)z_m}{H}\right)}{\cosh(z_m)}\right) \le \frac{1}{H}\left(\frac{\bar{\alpha}}{z_1}+1\right).$$

In the last inequality we used the fact that $\cosh\left((H-y_\ell)z_m\right) \le \cosh(z_m)$ for $y_\ell \in [0,H]$, $|\tanh(H-y_\ell)| \le 1$ for all $y_\ell \in [0,H]$, and $\frac{1}{\frac{\bar{\alpha}}{z_m}\tanh(z_m)+1} \le 1$. Then,

$$\left| \sum_{m=1}^{\infty} \frac{B_{n,m,1}^{(s,r)}}{z_m^{5/2}\psi_m(H)} \phi_m(x_\ell) \frac{\partial \psi_m}{\partial y_\ell}(H-y_\ell) \right|$$
$$\le \sum_{m=1}^{\infty} \frac{|B_{n,m,1}^{(s,r)}|}{z_m^{3/2}} \left(\frac{\bar{\alpha}}{z_1}+1\right) \frac{\left|\frac{\partial}{\partial y}\left(\psi_m(H-y_\ell)\right)\right|}{z_m|\psi_m(H)|}$$
$$\le \frac{1}{H}\left(\frac{\bar{\alpha}}{z_1}+1\right)^2 M_n^{(s,r)} \sum_{m=1}^{\infty} \frac{1}{z_m^{3/2}} < \infty.$$

Thus, the series in (B.1) converges uniformly in $[0,H]^2$ for $\sigma = (0,1)$.

Note that

$$\frac{\partial}{\partial x_\ell}\phi_m(x_\ell) = \frac{1}{H}\left[\bar{\alpha}\cos\left(\frac{z_m x_\ell}{H}\right) - z_m \sin\left(\frac{z_m x_\ell}{H}\right)\right] \le \frac{1}{H}\left(\bar{\alpha} + z_m\right).$$

Also $\psi_m(H-y_\ell) \le \psi_m(H)$ for y_ℓ in $[0,H]$. Then for $\sigma = (1,0)$ we have

$$\left| \sum_{m=1}^{\infty} \frac{\partial}{\partial x_\ell} \left(\frac{B_{n,m,1}^{(s,r)}}{z_m^{5/2}\psi_m(H)} \phi_m(x_\ell)\psi_m(H-y_\ell) \right) \right|$$
$$\le \sum_{m=1}^{\infty} M_n^{(s,r)} \frac{1}{H}\left(\frac{\bar{\alpha}}{z_m}+1\right)\frac{1}{z_m^{3/2}}$$

$$\leq M_n^{(s,r)} \frac{1}{H} \left(\frac{\bar{\alpha}}{z_1} + 1 \right) \sum_{m=1}^{\infty} \frac{1}{z_m^{3/2}} < \infty \, .$$

Hence, the series in (B.1) converges uniformly in $[0, H]^2$ for $\sigma = (1, 0)$.

We have that

$$\frac{\partial^2 \phi_m}{\partial x_\ell^2}(x_\ell) = \frac{1}{H^2} \left[-z_m \bar{\alpha} \sin(\frac{z_m x_\ell}{H}) - z_m^2 \cos(\frac{z_m x_\ell}{H}) \right] .$$

Note that another bound for $\psi_m(H - y_\ell)/\psi_m(H)$, tighter for large m, can be obtained as follows,

$$\begin{aligned}
\left| \frac{\psi_m(H - y_\ell)}{\psi_m(H)} \right| &= \frac{\frac{\bar{\alpha}}{z_m} \sinh\left(\frac{z_m(y_\ell - H)}{H}\right) + \cosh\left(\frac{z_m(y_\ell - H)}{H}\right)}{\psi_m(H)} \\
&= \frac{\frac{\bar{\alpha}}{z_m} \tanh\left(\frac{z_m(y_\ell - H)}{H}\right) + 1}{\left[\frac{\bar{\alpha}}{z_m} \tanh(z_m) + 1\right]} \left(\frac{\cosh\left(\frac{z_m(y_\ell - H)}{H}\right)}{\cosh(z_m)} \right) \\
&\leq \left(\frac{\bar{\alpha}}{z_1} + 1 \right) \left(\frac{\cosh\left(\frac{z_m(y_\ell - H)}{H}\right)}{\cosh(z_m)} \right) ,
\end{aligned}$$

and for $y_\ell \in (0, H)$,

$$\begin{aligned}
\frac{\cosh\left(\frac{z_m(H - y_\ell)}{H}\right)}{\cosh(z_m)} &= \frac{1 + e^{-2\left(\frac{z_m(H - y_\ell)}{H}\right)}}{1 + e^{-2z_m}} e^{z_m \frac{(H - y_\ell)}{H} - z_m} \\
&= \frac{1 + e^{-2\left(\frac{z_m(H - y_\ell)}{H}\right)}}{1 + e^{-2z_m}} e^{\frac{-z_m y_\ell}{H}} \leq 2 \frac{1}{z_m^2 \left(\frac{y_\ell}{H}\right)^2} \, .
\end{aligned}$$

Thus,

$$\left| \frac{\psi_m(H - y_\ell)}{\psi_m(H)} \right| \leq \left(\frac{\bar{\alpha}}{z_1} + 1 \right) \left(2 \frac{1}{z_m^2 \left(\frac{y_\ell}{H}\right)^2} \right) . \tag{B.2}$$

Then we have for $\sigma = (2, 0)$ and $0 < \epsilon < y_\ell < H$ that

$$\begin{aligned}
&\sum_{m=1}^{\infty} \frac{\partial^2}{\partial x_\ell^2} \left(\frac{B_{n,m,1}^{(s,r)}}{z_m^{5/2} \psi_m(H)} \phi_m(x_\ell) \psi_m(H - y_\ell) \right) \\
&= \sum_{m=1}^{\infty} \frac{B_{n,m,1}^{(s,r)}}{z_m^{5/2}} \frac{1}{H^2} \left[z_m \sin(\frac{z_m x_\ell}{H}) - z_m^2 \cos(\frac{z_m x_\ell}{H}) \right] \frac{\psi_m(H - y_\ell)}{\psi_m(H)} \\
&\leq \sum_{m=1}^{\infty} \frac{B_{n,m,1}^{(s,r)}}{z_m^{5/2}} \frac{1}{H^2} \left| z_m \sin(\frac{z_m x_\ell}{H}) - z_m^2 \cos(\frac{z_m x_\ell}{H}) \right| \left(\frac{\bar{\alpha}}{z_1} + 1 \right) \left(2 \frac{1}{z_m^2 \left(\frac{y_\ell}{H}\right)^2} \right) \\
&\leq 2 \frac{M_n^{(s,r)}}{\epsilon^2} \left(\frac{1}{z_1} + 1 \right) \left(\frac{\bar{\alpha}}{z_1} + 1 \right) \sum_{m=1}^{\infty} \frac{1}{z_m^{5/2}} < \infty.
\end{aligned}$$

Consequently, the series in (B.1) converges uniformly in $(0, H) \times (\epsilon, H)$ for $\sigma = (2, 0)$.

Now we analyze the case $\sigma = (0,2)$. We have that, using (B.2),

$$\left|\frac{\frac{d^2}{dy_\ell^2}(\psi_m(H-y_\ell))}{\frac{\bar\alpha}{H}\sinh(z_m)+\cosh(z_m)}\right| = \left|\frac{z_m^2}{H^2}\frac{\psi_m(H-y_\ell)}{\frac{\bar\alpha}{H}\sinh(z_m)+\cosh(z_m)}\right|$$
$$\leq \frac{z_m^2}{H^2}\left(\frac{\bar\alpha}{z_1}+1\right)\left(\frac{2}{z_m^2\left(\frac{y_\ell}{H}\right)^2}\right) = \left(\frac{\bar\alpha}{z_1}+1\right)\left(\frac{2}{y_\ell^2}\right).$$

Then, for $\sigma = (0,2)$ and $0 < \epsilon < y_\ell < H$, we have

$$\begin{aligned}
&\sum_{m=1}^{\infty}\frac{\partial^2}{\partial y_\ell^2}\left(\frac{B_{n,m,1}^{(s,r)}\phi_m(x_\ell)\psi_m(H-y_\ell)}{z_m^{5/2}\psi_m(H)}\right)\\
&\quad= \sum_{m=1}^{\infty}\frac{B_{n,m,1}^{(s,r)}}{z_m^{5/2}}\phi_m(x_\ell)\frac{\left(\frac{d^2}{dy_\ell^2}(\psi_m(H-y_\ell))\right)}{\psi_m(H)}\\
&\quad\leq \sum_{m=1}^{\infty}\frac{M_n^{(s,r)}}{z_m^{5/2}}\left(\frac{\bar\alpha}{z_1}+1\right)\left(\frac{\bar\alpha}{z_1}+1\right)\left(\frac{2}{y_\ell^2}\right)\\
&\quad\leq M_n^{(s,r)}\left(\frac{\bar\alpha}{z_1}+1\right)^2\frac{2}{\epsilon^2}\sum_{m=1}^{\infty}z_m^{5/2} < \infty.
\end{aligned}$$

Thus, the series in (B.1) converges uniformly in $(0,H)\times(\epsilon,H)$ for $\sigma = (0,2)$. Note that the summation sign and the integral of a series commute if the series converges absolutely. In the proof of part 1 we have shown that (B.1) converges absolutely and uniformly in $[0,H]^2$ when $\sigma = (1,0)$ and $\sigma = (0,1)$. From this fact, part 3 of the lemma follows, and the proof is complete. ∎

Appendix C. Proof of Theorem 3.2.

For the proof of Theorem 3.2, we will use the following intermediate result on the rate of decay of the coefficients of the series expansion of C^2-functions in terms of the basis functions defined by (3.8) with respect to the roots (3.11).

LEMMA C.1. *Let $M > 0$ and $g : [0,H] \to \mathbb{R}$ be such that $g \in C^2((0,H))$, $\frac{d^\sigma g}{dx_\ell^\sigma}(x_\ell) \leq M$, for all $x_\ell \in (0,H)$ and for $\sigma = 0,1,2$, and $\lim_{x_\ell\to 0}\frac{d^\sigma g}{dx_\ell^\sigma}(x_\ell) < M$ and $\lim_{x_\ell\to H}\frac{d^\sigma g}{dx_\ell^\sigma}(x_\ell) < M$ for $\sigma = 0,1$. Let us define C_m as the coefficients of the expansion of $g(x)$ in the basis given by $\{\phi_m\}_{m\in\mathbb{N}}$, i.e.,*

$$g(x_\ell) = \sum_{m=1}^{\infty} C_m\phi_m(x_\ell).$$

Then, the coefficients C_m can be written as

$$C_m = \frac{\bar C_m}{z_m^2}, \qquad \text{with} \quad |\bar C_m| \leq K,$$

for some $K > 0$ and for all $m \in \mathbb{N}$.

Proof. Since $\{\phi_m\}_{m\in\mathbb{N}}$ is a complete orthogonal set, we have that

$$C_m = \frac{\int_0^H g(x_\ell)\phi_m(x_\ell)dx_\ell}{\int_0^H \phi_m^2(x_\ell)dx_\ell} = \frac{\int_0^H g(x_\ell)\left(\frac{\bar\alpha}{z_m}\sin\left(\frac{z_m x_\ell}{H}\right)+\cos\left(\frac{z_m x_\ell}{H}\right)\right)dx_\ell}{\int_0^H\left(\frac{\bar\alpha}{z_m}\sin\left(\frac{z_m x_\ell}{H}\right)+\cos\left(\frac{z_m x_\ell}{H}\right)\right)^2 dx_\ell}.$$

We first look at the numerator. Using integration by parts, we have

$$\begin{aligned}\int_0^H \frac{\bar{\alpha}}{z_m}\sin\left(\frac{z_m x_\ell}{H}\right) g(x_\ell)dx_\ell \\ = \frac{\bar{\alpha}H}{z_m^2}\left[-g(H)\cos(z_m)+g(0)+\int_0^H \cos\left(\frac{z_m x_\ell}{H}\right)\frac{\partial g}{\partial x_\ell}(x_\ell)dx_\ell\right]\end{aligned} \tag{C.1}$$

and

$$\begin{aligned}&\int_0^H \cos\left(\frac{z_m x_\ell}{H}\right) g(x_\ell)dx_\ell \\ &= \frac{H}{z_m}\left[g(H)\sin(z_m)-\int_0^H \sin\left(\frac{z_m x_\ell}{H}\right)\frac{\partial g}{\partial x_\ell}(x_\ell)dx_\ell\right] \\ &= \frac{H}{z_m}g(H)\sin(z_m) \\ &\quad -\left(\frac{H}{z_m}\right)^2\left[-\frac{\partial g}{\partial x_\ell}(H)\cos(z_m)+\frac{\partial g}{\partial x_\ell}(0)\right. \\ &\qquad\qquad \left.+\int_0^H \cos\left(\frac{z_m x_\ell}{H}\right)\frac{\partial^2 g}{\partial x_\ell^2}(x_\ell)dx_\ell\right] \\ &= \frac{H}{z_m}g(H)\frac{z_m\sin(z_m)}{z_m} \\ &\quad -\left(\frac{H}{z_m}\right)^2\left[-\frac{\partial g}{\partial x_\ell}(H)\cos(z_m)+\frac{\partial g}{\partial x_\ell}(0)\right. \\ &\qquad\qquad \left.+\int_0^H \cos\left(\frac{z_m x_\ell}{H}\right)\frac{\partial^2 g}{\partial x_\ell^2}(x_\ell)dx_\ell\right].\end{aligned} \tag{C.2}$$

Using (C.1) and (C.2), we have

$$\begin{aligned}&\int_0^H g(x_\ell)\left[\frac{\bar{\alpha}}{z_m}\sin\left(\frac{z_m x_\ell}{H}\right)+\cos\left(\frac{z_m x_\ell}{H}\right)\right]dx_\ell \\ &= \frac{\bar{\alpha}H}{z_m^2}\left[-g(H)\cos(z_m)+g(0)+\int_0^H \cos\left(\frac{z_m x_\ell}{H}\right)\frac{\partial g}{\partial x_\ell}(x_\ell)dx_\ell\right] \\ &\quad + g(H)H\frac{z_m\sin(z_m)}{z_m^2} \\ &\quad -\left(\frac{H}{z_m}\right)^2\left[-\frac{\partial g}{\partial x_\ell}(H)\cos(z_m)+\frac{\partial g}{\partial x_\ell}(0)\right. \\ &\qquad\qquad \left.+\int_0^H \cos\left(\frac{z_m x_\ell}{H}\right)\frac{\partial^2 g}{\partial x_\ell^2}(x_\ell)dx_\ell\right]\end{aligned}$$

$$
\begin{aligned}
= \frac{1}{z_m^2}\Bigg\{ & \bar{\alpha} H \left[-g(H)\cos(z_m) + g(0) + \int_0^H \cos\left(\frac{z_m x_\ell}{H}\right) \frac{\partial g}{\partial x_\ell}(x_\ell) dx_\ell \right] \\
& + g(H) H z_m \sin(z_m) \\
& - \left(H^2\right) \Bigg[-\frac{\partial g}{\partial x_\ell}(H)\cos(z_m) + \frac{\partial g}{\partial x_\ell}(0) \\
& \qquad + \int_0^H \cos\left(\frac{z_m x_\ell}{H}\right) \frac{\partial^2 g}{\partial x_\ell^2}(x_l) dx_\ell \Bigg] \Bigg\} := \frac{1}{z_m^2} N_m.
\end{aligned} \tag{C.3}
$$

Then, from the last identity, it follows that we can write $C_m = \bar{C}_m / z_m^2$, where $\bar{C}_m = N_m / D_m$, with

$$
D_m = \int_0^H \left[\frac{\bar{\alpha}}{z_m} \sin\left(\frac{z_m x_\ell}{H}\right) + \cos\left(\frac{z_m x_\ell}{H}\right) \right]^2 dx_\ell \, .
$$

We now show that $|\bar{C}_m| < K$ for some K. By simply evaluating the integral and rearranging the resulting expression, we have that

$$
D_m = \frac{H\left(-\bar{\alpha}^2 \sin(2z_m) + 2\bar{\alpha} z_m \left(\bar{\alpha} - \cos(2z_m) + 1\right) + z_m^2 \sin(2z_m)\right)}{4 z_m^3} + \frac{H}{2} \, . \tag{C.4}
$$

Note that $D_m > 0$ for all $m \in \mathbb{N}$ and that the first term in (C.4) goes to zero as m goes to infinity since $z_m \to \infty$ as $m \to \infty$. Then, there exist an $\hat{m}$ such that for all $m \geq \hat{m}$ we have $D_m \geq H/4$. Let

$$
\omega = \min \left\{ \min_{m \in \{1,\ldots,\hat{m}\}} D_m, \frac{H}{2} \right\} \, .
$$

Then, $\omega > 0$ (since it is the minimum of a finite set of positive numbers), and for all $m \in \mathbb{N}$, we have $D_m \geq \omega$, and thus,

$$
\frac{1}{D_m} \leq \frac{1}{\omega} < \infty. \tag{C.5}
$$

We turn now to the bound of N_m as defined in (C.3). By hypothesis, we have that there exists an $M > 0$ such that

$$
g(H^-),\ g(0^+),\ \frac{dg}{dx_\ell}(H^-),\ \frac{dg}{dx_\ell}(0^+) < M < \infty \quad \text{and} \quad \frac{d^2 g}{dx_\ell^2} \leq M \quad \text{in } (0, H).
$$

We next wish to bound $|z_m \sin(z_m)|$, and we will use the property (3.11). To that end, we consider two possible cases, depending on whether $z_m = \bar{\alpha}$ or not. If there exists an $m_{\bar{\alpha}} \in \mathbb{N}$ such that $z_{m_{\bar{\alpha}}} = \bar{\alpha}$, then we have from (3.10) since $\bar{\alpha} > 0$ that $\cos(z_{m_{\bar{\alpha}}}) = 0$. This implies that $z_{m_{\bar{\alpha}}} = (2j-1)\pi/2$ for some $j \in \mathbb{N}$. Then, it follows that $|\sin(z_{m_{\bar{\alpha}}})| = 1$. Consequently,

$$
|z_{m_{\bar{\alpha}}} \sin(z_{m_{\bar{\alpha}}})| = \bar{\alpha}.
$$

For $\bar{\alpha} > 0$ such that $\bar{\alpha} \neq z_m$ for all $m \in \mathbb{N}$, we can write (again from (3.10))

$$
\sin(z_m) = \frac{2 z_m \bar{\alpha}}{\bar{\alpha}^2 - z_m^2} \cos(z_m).
$$

Let $z_{\min} \in \{z_m\}$ such that $|z_{\min}^2 - \bar{\alpha}^2| = \min_{m\in\mathbb{N}} |z_m^2 - \bar{\alpha}^2|$. Then,

$$|z_m \sin(z_m)| = \left|\frac{2z_m^2\bar{\alpha}\cos(z_m)}{\bar{\alpha}^2 - z_m^2}\right| = \left|\frac{2\bar{\alpha}\cos(z_m)}{\left(\frac{\bar{\alpha}}{z_m}\right)^2 - 1}\right| \leq \frac{2\bar{\alpha}}{\left|\left(\frac{\bar{\alpha}}{z_{\min}}\right)^2 - 1\right|}\,.$$

Let us define

$$Q := \begin{cases} \bar{\alpha}, & \text{if } (2\bar{\alpha}+\pi)/(2\pi) \in \mathbb{N}, \\ \frac{2\bar{\alpha}}{(\bar{\alpha}/z_{\min})^2 - 1}, & \text{otherwise.} \end{cases}$$

Then, for all $\bar{\alpha} > 0$ we have

$$|N_m| \leq \bar{\alpha}\,[2M + MH]\,H + MHQ + H^2\,[2M + HM]\,. \tag{C.6}$$

Thus, from (C.5) and (C.6), we have that for all $m \in \mathbb{N}$

$$|\bar{C}_m| = \left|\frac{N_m}{D_m}\right| \leq \frac{M}{\omega}\left\{\bar{\alpha}\,(2+H)\,H + HQ + H^2\,(2+H)\right\} := K < \infty,$$

i.e., $\bar{C}_m$ is uniformly bounded for all $m \in \mathbb{N}$. $\square$

We present now the proof of the theorem.

Proof of Theorem 3.2. We present in detail the proof for the case $i = 1$, but a similar procedure can be applied for the cases $i = 2, 3, 4$, and therefore these are omitted for brevity. We use induction in n. Let us first consider the case $n = 1$.

Let

$$g_{0,1}(x_\ell) := \left(-\frac{\partial}{\partial y_\ell}\eta_0^{(s,r-1)} + \alpha\eta_0^{(s,r-1)}\right)(x_\ell, H - 2\gamma), \tag{C.7}$$

i.e., $g_{0,1}$ is the right-hand side of the non-homogeneous boundary condition from the equations defining one of the four components of the error at step $n = 1$, with $\eta_{1,1}^{(s,r)}$ as in (3.2). By hypothesis, the initial approximation u_0 is such that the initial error η_0 is piecewise C^3 in Ω (e.g., $u_0 = 0$ when $f \in C^1(\Omega)$). Then, $g_{0,1}$ satisfies the hypothesis of Lemma C.1.

Consequently, by Lemma C.1 there exist $\{C_{1,m,1}^{(s,r)}\}_{m\in\mathbb{N}}$ and $\{\bar{C}_{1,m,1}^{(s,r)}\}_{m\in\mathbb{N}}$ such that

$$g_{0,1}(x_\ell) = \sum_{m=1}^{\infty} C_{1,m,1}^{(s,r)}\phi_m(x_\ell), \qquad \text{where} \quad C_{1,m,1}^{(s,r)} = \frac{\bar{C}_{1,m,1}^{(s,r)}}{z_m^2}\,,$$

with $\left\{\bar{C}_{1,m,1}^{(s,r)}\right\}_{m\in\mathbb{N}}$ uniformly bounded in $m \in \mathbb{N}$. Using these bounded sequences we are ready to construct the coefficients for (3.14) so that the generalized Fourier series (3.14) is the solution of the equation for the error (3.2). To that end, let us define

$$B_{1,m,1}^{(s,r)} = \frac{z_m^{1/2}\bar{C}_{1,m,1}^{(s,r)}\psi_m(H)}{\frac{d\psi_m}{dy_\ell}(H) + \alpha\psi_m(H)}\,. \tag{C.8}$$

To bound these coefficients, we use that $\bar{\alpha} > 0$, $\tanh(z_m) < 1$, for all $m \in \mathbb{N}$, the fact that $0 < z_1 < z_2 < \cdots$, and that $0 < \tanh(z_1) < \tanh(z_2) < \cdots$ to obtain

$$\frac{\psi_m(H)}{\frac{d\psi_m}{dy_\ell}(H) + \alpha\psi_m(H)} = \frac{\left[\frac{\bar{\alpha}}{z_m}\sinh(z_m) + \cosh(z_m)\right]}{\left(z_m + \frac{\bar{\alpha}^2}{z_m}\right)\sinh(z_m) + 2\bar{\alpha}\cosh(z_m)}$$

$$= \frac{\frac{\bar{\alpha}}{z_m}\tanh(z_m)+1}{z_m\left[\left(1+\left(\frac{\bar{\alpha}}{z_m}\right)^2\right)\tanh(z_m)+\frac{2\bar{\alpha}}{z_m}\right]} \leq \frac{\frac{\bar{\alpha}}{z_m}\tanh(z_m)+1}{z_m\tanh(z_m)}$$

$$\leq \frac{1}{z_m}\left(\frac{\bar{\alpha}}{z_m}+\frac{1}{\tanh(z_m)}\right) \leq \frac{1}{z_m}\left(\frac{\bar{\alpha}}{z_1}+\frac{1}{\tanh(z_1)}\right).$$

Thus, with $M_1^{(s,r)} = \bar{C}_{1,m,1}^{(s,r)}\left(\bar{\alpha}/z_1 + 1/\tanh(z_1)\right)/z_1^{1/2}$ we have

$$|B_{1,m,1}^{(s,r)}| \leq \frac{z_m^{1/2}\bar{C}_{1,m,1}^{(s,r)}\left(\frac{\bar{\alpha}}{z_1}+\frac{1}{\tanh(z_1)}\right)}{z_m} \leq \frac{\bar{C}_{1,m,1}^{(s,r)}\left(\frac{\bar{\alpha}}{z_1}+\frac{1}{\tanh(z_1)}\right)}{z_1^{1/2}} = M_1^{(s,r)} \tag{C.9}$$

for all $m \in \mathbb{N}$. That is, the coefficients $B_{1,m,1}^{(s,r)}$ as in (C.8) satisfy (3.18) for $n = 1$.

Let us define the function $\upsilon : [0,H]^2 \to \mathbb{R}$ as

$$\upsilon(x_\ell, y_\ell) = \sum_{m=1}^{\infty} \frac{B_{1,m,1}^{(s,r)}}{z_m^{5/2}\psi_m(H)}\phi_m(x_\ell)\psi_m(H-y_\ell).$$

We shall show that υ solves the equations that define $\eta_{1,1}^{(s,r)}$, i.e., it solves (3.2) for $n = 1$. Let $\sigma = (\sigma_1, \sigma_2)$ be a multi-index. Then, we have $\partial^\sigma = \frac{\partial^{\sigma_1}}{\partial x}\frac{\partial^{\sigma_2}}{\partial y}$. In Appendix B it is shown that the identity

$$\partial^\sigma \sum_{m=1}^{\infty} \frac{B_{1,m,1}^{(s,r)}}{z_m^{5/2}\psi_m(H)}\phi_m(x_\ell)\psi_m(H-y_\ell) = \sum_{m=1}^{\infty} \partial^\sigma \frac{B_{1,m,1}^{(s,r)}}{z_m^{5/2}\psi_m(H)}\phi_m(x_\ell)\psi_m(H-y_\ell)$$

holds in $[0,H]^2$ for $\sigma = (1,0), \sigma = (0,1)$ and in $(0,H)^2$ for $\sigma = (2,0), \sigma = (0,2)$, i.e., the order of infinite summation and differentiation commutes for the derivative of the series expansion of υ.

Then, since by Lemma 3.1, $\Delta(\phi_m(x_\ell)\psi_m(H-y_\ell)) = 0$ in $(0,H)^2$ and the order of derivatives and summation commute, we have that

$$\Delta\upsilon(x_\ell, y_\ell) = \sum_{m=1}^{\infty} \frac{B_{n+1,m,i}^{(s,r)}\Delta(\phi_m(x_\ell)\psi_m(H-y_\ell))}{z_m^{5/2}\psi_m(H)} = 0.$$

Also,

$$\left(-\frac{\partial}{\partial x_\ell}+\alpha\right)\upsilon(0,y_\ell) = \sum_{m=1}^{\infty} \frac{B_{1,m,1}^{(s,r)}\left(-\frac{d\phi_m}{dx_\ell}+\alpha\phi_m\right)(0)\psi_m(y_\ell)}{z_m^{5/2}\psi_m(H)} = 0,$$

since by the second equation in (3.6), $\left(-\frac{d\phi_m}{dx_\ell}+\alpha\phi_m\right)(0) = 0$,

$$\left(\frac{\partial}{\partial x_\ell}+\alpha\right)\upsilon(H,y_\ell) = \sum_{m=1}^{\infty} \frac{B_{1,m,1}^{(s,r)}\left(\frac{d\phi_m}{dx_\ell}+\alpha\phi_m\right)(H)\psi_m(y_\ell)}{z_m^{5/2}\psi_m(H)} = 0,$$

since by the third equation in (3.6), $\left(\frac{d\phi_m}{dx_\ell}+\alpha\phi_m\right)(H) = 0$, and

$$\left(\frac{\partial}{\partial y_\ell}+\alpha\right)\upsilon(x_\ell,H) = \sum_{m=1}^{\infty} \frac{B_{1,m,1}^{(s,r)}\left(\frac{-d\psi_m}{dy_\ell}+\alpha\psi_m\right)(0)}{z_m^{5/2}\psi_m(H)}\phi_m(x_\ell) = 0,$$

since by the second equation in (3.7), $\left(\frac{-d\psi_m}{dy_\ell} + \alpha\psi_m\right)(0) = 0$.

Thus, we have that υ satisfies Laplace's equation in $(0, H)^2$ and the three homogeneous boundary conditions from the definition of $\eta_{1,1}^{(s,r)}$. It remains to verify that υ satisfies the non-homogeneous boundary condition at the bottom boundary, i.e., at $y_\ell = 0$. Note that

$$\left(-\frac{\partial}{\partial y_\ell} + \alpha\right)\upsilon(x_\ell, y_\ell) = \sum_{m=1}^{\infty} \frac{B_{n+1,m,i}^{(s,r)}\left(\frac{d\psi_m}{dy_\ell} + \alpha\psi_m\right)(H - y_\ell)}{z_m^{5/2}\psi_m(H)}\phi_m(x_\ell).$$

Then for $y_\ell = 0$ and $n = 1$ we have

$$\begin{aligned}\left(-\frac{\partial}{\partial y_\ell} + \alpha\right)\upsilon(x_\ell, 0) &= \sum_{m=1}^{\infty} \frac{B_{1,m,1}^{(s,r)}\phi_m(x_\ell)\left(\frac{d\psi_m}{dy_\ell} + \alpha\psi_m\right)(H)}{z_m^{5/2}\psi_m(H)} \\ &= \sum_{m=1}^{\infty} \frac{\bar{C}_{1,m,1}^{(s,r)}}{z_m^2}\phi_m(x_\ell) = \sum_{m=1}^{\infty} C_{1,m,1}^{(s,r)}\phi_m(x_\ell) \\ &= g_{0,1}(x_\ell) = \left(-\frac{\partial}{\partial y_\ell}\eta_0^{s,r-1} + \alpha\eta_0^{s,r-1}\right)(x_\ell, H - 2\gamma),\end{aligned}$$

where in the second equality we used (C.8) and in the last equality we used (C.7). Thus, υ solves the equations defining $\eta_{1,1}^{(s,r)}$. Consequently, $\eta_{1,1}^{(s,r)} = \upsilon$ and (3.14) holds with $|B_{1,m,1}^{(s,r)}| \le M_1^{(s,r)}$ for some $M_1^{(s,r)} > 0$. Hence, the case $n = 1$ is proved.

Next we show that if the series expansions (3.14)–(3.17) hold for the error at step n with (3.18), then the same holds for step $n + 1$. To that end, let

$$g_{n,1}(x_\ell) = \left(-\frac{\partial}{\partial y_\ell} + \alpha\right)\eta_n^{(s,r-1)}(x_\ell, H - 2\gamma)\ , \tag{C.10}$$

i.e., $g_{n,1}$ is the right-hand side of the non-homogeneous boundary condition from the equations defining $\eta_{n+1,1}^{(s,r)}$ as in (3.2). Let us define $C_{n,m,1}^{(s,r)}$ as the coefficients of the expansion of $g_{n,1}(x_\ell)$ in the basis given by $\{\phi_m\}_{m\in\mathbb{N}}$, where $\phi_m(x_\ell)$ is as in (3.8). Thus,

$$g_{n,1}(x_\ell) = \sum_{m=1}^{\infty} C_{n,m,1}^{(s,r)}\phi_m(x_\ell)$$

and

$$C_{n,m,1}^{(s,r)} = \frac{\int_0^H g_{n,1}(x_\ell)\phi_m(x_\ell)dx_\ell}{\int_0^H \phi_m^2(x_\ell)dx_\ell}\ . \tag{C.11}$$

Note that, unlike the first iteration, we do not know the regularity of $g_{n,1}$ (even if $g_{n,1}$ is harmonic in the interior of the subdomain, this does not imply that it will necessarily be twice differentiable on the boundaries of the subdomain). Therefore, we cannot use integration by parts and Lemma C.1 to conclude that $C_{n,m,1}^{(s,r)}$ decays like $1/z_m^2$. This is precisely why we have to use induction.

Let us define

$$B_{n+1,m,1}^{(s,r)} = \frac{C_{n,m,1}^{(s,r)} z_m^{5/2}\psi_m(H)}{\frac{d\psi_m}{dy_\ell}(H) + \alpha\psi_m(H)}\ . \tag{C.12}$$

Then, from (C.11) and (C.12) we obtain

$$B^{(s,r)}_{n+1,m,1} = \left(\frac{\int_0^H g_{n,1}(x_\ell)\phi_m(x_\ell)dx_\ell}{\int_0^H \phi_m^2(x_\ell)dx_\ell} \right) \frac{z_m^{5/2}\psi_m(H)}{\frac{d\psi_m}{dy_\ell}(H) + \alpha\psi_m(H)} . \tag{C.13}$$

We shall see that these are indeed the coefficients we need in (3.14), i.e., with these coefficients, the expansion (3.14) satisfies (3.2). We have to prove first that $|B^{(s,r)}_{n+1,m,i}| \leq M^{(s,r)}_{n+1}$ for all $m \in \mathbb{N}$ and some $M^{(s,r)}_{n+1} > 0$. This result is necessary to guarantee the interchange of summation and differentiation of a series that is defined later. We can write the error in the subdomain $(s, r-1)$ at step n in terms of its four parts defined in (3.2)–(3.5), i.e.,

$$\eta_n^{(s,r-1)}(x_\ell, y_\ell) = \sum_{i=1}^{4} \eta_{n,i}^{(s,r-1)}(x_\ell, y_\ell).$$

Plugging this expression into (C.10) we obtain

$$\begin{aligned} g_{n,1}(x_\ell) &= \left(-\frac{\partial}{\partial y_\ell} + \alpha\right) \eta_n^{s,r-1}(x_\ell, H-2\gamma) \\ &= \sum_{i=1}^{4} \left(-\frac{\partial}{\partial y_\ell} + \alpha\right) \eta_{n,i}^{(s,r-1)}(x_\ell, H-2\gamma). \end{aligned} \tag{C.14}$$

By the induction hypothesis we have that $\eta_{n,i}^{(s,r-1)}$, $i = 1, 2, 3, 4$, is given by the series in (3.14)–(3.17) with $|B^{(s,r-1)}_{n,m,i}| \leq M^{(s,r)}_n$.

We want to look at the expression of a particular but generic coefficient, say, $B^{(s,r)}_{n+1,k,1}$. To that end, we multiply both sides of (C.14) by $\phi_k(x_\ell)$ and integrate over $[0, H]$ to obtain

$$\begin{aligned} &\int_0^H g_{n,1}(x_\ell)\phi_k(x_\ell)dx_\ell \\ &= \int_0^H \left(\sum_{i=1}^{4} \left(-\frac{\partial}{\partial y_\ell} + \alpha\right) \eta_{n,i}^{s,r-1}(x_\ell, H-2\gamma) \right) \phi_k(x_\ell)dx_\ell \\ &= \sum_{m=1}^{\infty} \frac{B^{(s,r-1)}_{n,m,1}}{z_m^{5/2}\psi_m(H)} \int_0^H \phi_m(x_\ell)\phi_k(x_\ell)dx_\ell \left(\frac{d\psi_m}{dy_\ell} + \alpha\psi_m \right)(2\gamma) \\ &\quad + \sum_{m=1}^{\infty} \frac{B^{(s,r-1)}_{n,m,2}}{z_m^{5/2}\psi_m(H)} \int_0^H \psi_m(x_\ell)\phi_k(x_\ell)dx_\ell \left(\frac{-d\phi_m}{dy_\ell} + \alpha\phi_m \right)(H-2\gamma) \\ &\quad + \sum_{m=1}^{\infty} \frac{B^{(s,r-1)}_{n,m,3}}{z_m^{5/2}\psi_m(H)} \int_0^H \phi_m(x_\ell)\phi_k(x_\ell)dx_\ell \left(\frac{-d\psi_m}{dy_\ell} + \alpha\psi_m \right)(H-2\gamma) \\ &\quad + \sum_{m=1}^{\infty} \frac{B^{(s,r-1)}_{n,m,4}}{z_m^{5/2}\psi_m(H)} \int_0^H \psi_m(H-x_\ell)\phi_k(x_\ell)dx_\ell \left(\frac{-d\phi_m}{dy_\ell} + \alpha\phi_m \right)(H-2\gamma). \end{aligned} \tag{C.15}$$

Note that we have interchanged the order of the summation, derivatives, and integrals in the right-hand side of the above equation. The justification for these order interchanges is given in Appendix B.

Let $\bar{\gamma} = \gamma/H$ be the normalized overlap. Plugging (C.15) into (C.13) and evaluating the integrals we obtain the following expression[4]

(C.16)

$$
\begin{aligned}
&B^{(s,r)}_{n+1,k,1} \\
&= \frac{\left(z_k + \frac{\bar{\alpha}^2}{z_k}\right)\sinh\left(2\bar{\gamma}z_k\right) + 2\bar{\alpha}\cosh\left(2\bar{\gamma}z_k\right)}{\left(z_k + \frac{\bar{\alpha}^2}{z_k}\right)\sinh\left(z_k\right) + 2\bar{\alpha}\cosh\left(z_k\right)} B^{(s,r-1)}_{n,k,1} \\
&\quad + \sum_{m=1}^{\infty} \left\{ \frac{4z_k^{11/2}\left[\frac{\bar{\alpha}}{z_k}\tanh(z_k)+1\right]\left(z_m + \frac{\bar{\alpha}^2}{z_m}\right)\sin\left((1-2\bar{\gamma})z_m\right)}{z_m^{1/2}\left[\left(z_k + \frac{\bar{\alpha}^2}{z_k}\right)\tanh(z_k) + 2\bar{\alpha}\right] z_m^2\left(z_m z_k^3 + z_k z_m^3\right)} \right. \\
&\quad \times \left. \frac{\left\{\tanh(z_m)\left[\bar{\alpha}(z_k^2+z_m^2)\sin(z_k) - z_k(\bar{\alpha}^2 - z_m^2)\cos(z_k)\right] + z_m(\bar{\alpha}^2+z_k^2)\sin(z_k)\right\}}{\left[\frac{\bar{\alpha}}{z_m}\tanh(z_m)+1\right]\left[(z_k^2-\bar{\alpha}^2)\sin(2z_k) + 2z_k(\bar{\alpha}^2+z_k^2+\bar{\alpha}) - 2\bar{\alpha}z_k\cos(2z_k)\right]} B^{(s,r-1)}_{n,m,2} \right\} \\
&\quad + \frac{\left(-z_k + \frac{\bar{\alpha}^2}{z_k}\right)\sinh\left((1-2\bar{\gamma})z_k\right)}{\left(z_k + \frac{\bar{\alpha}^2}{z_k}\right)\sinh\left(z_k\right) + 2\bar{\alpha}\cosh\left(z_k\right)} B^{(s,r-1)}_{n,k,3} \\
&\quad + \sum_{m=1}^{\infty} \left\{ \frac{4z_k^{11/2}\left[\frac{\bar{\alpha}}{z_k}\tanh(z_k)+1\right]\left(z_m + \frac{\bar{\alpha}^2}{z_m}\right)\sin\left((1-2\bar{\gamma})z_m\right)}{z_m^{1/2}\left[\left(z_k + \frac{\bar{\alpha}^2}{z_k}\right)\tanh(z_k) + 2\bar{\alpha}\right] z_m^2\left(z_m z_k^3 + z_k z_m^3\right)} \right. \\
&\quad \times \left. \frac{\left\{\tanh(z_m) z_k(\bar{\alpha}^2+z_m^2) - z_m\left[-2\bar{\alpha}z_k + \frac{(\bar{\alpha}^2 - z_k^2)\sin(z_k) + 2\bar{\alpha}z_k\cos(z_k)}{\cosh(z_m)}\right]\right\}}{\left[\frac{\bar{\alpha}}{z_m}\tanh(z_m)+1\right]\left[(z_k^2-\bar{\alpha}^2)\sin(2z_k) + 2z_k(\bar{\alpha}^2+z_k^2+\bar{\alpha}) - 2\bar{\alpha}z_k\cos(2z_k)\right]} B^{(s,r-1)}_{n,m,4} \right\}.
\end{aligned}
$$

In Appendix D it is shown that $B^{(s,r)}_{n+1,k,1}$ defined by (C.16) satisfies the inequality $|B^{(s,r)}_{n+1,k,1}| \leq M^{(s,r)}_{n+1}$ for some $M^{(s,r)}_{n+1} > 0$ for all $k \in \mathbb{N}$. Now, let

$$\bar{\upsilon}(x_\ell, y_\ell) = \sum_{m=1}^{\infty} \frac{B^{(s,r)}_{n+1,m,i}}{z_m^{5/2}\psi_m(H)} \phi_m(x_\ell)\psi_m(y_\ell).$$

By a similar reasoning as done before for υ, we can see that $\bar{\upsilon}$ solves all the equations defining $\eta^{(s,r)}_{n+1,1}$. Consequently, $\eta^{(s,r)}_{n+1,1} = \bar{\upsilon}$. Therefore,

$$\eta^{(s,r)}_{n+1,1} = \bar{\upsilon}(x_\ell, y_\ell) = \sum_{m=1}^{\infty} \frac{B^{(s,r)}_{n+1,m,i}}{z_m^2\psi_m(H)} \phi_m(x_\ell)\psi_m(H - y_\ell).$$

Thus, we just showed that if (3.14)–(3.17) and (3.18) hold for step n, then (3.14) and (3.18) with $i = 1$ hold for step $n+1$. The same result can be obtained with the same procedure for $\eta^{(s,r)}_{n,i}$ with $i = 2, 3, 4$. Therefore, if (3.14)–(3.17) and (3.18) hold for step n, then they hold for $n+1$, and the proof is complete. ∎

Appendix D. A uniform bound for the coefficients of the generalized Fourier series representation of the error.

THEOREM D.1. *Let the hypotheses of Theorem 3.2 hold. The coefficients* $B^{(s,r)}_{n+1,k,1}$ *defined in* (C.16) *are such that*

$$|B^{(s,r)}_{n+1,k,1}| \leq M^{(s,r)}_{n+1} \tag{D.1}$$

[4]We develop this formula, as well as those for all the other coefficients $B^{(s,r)}_{n+1,k,i}$ and therefore all the entries of the infinite matrix $\hat{T}$ defined in Section 3, with the aid of the program Mathematica.

for some $M_{n+1}^{(s,r)} > 0$ *and all* $k \in \mathbb{N}$.

Proof. We prove (D.1) by induction in n. For $n = 1$, this is shown in (C.9). So, we assume this expression holds for n, that is, $|B_{n,k,1}^{(s,r)}| \leq M_n^{(s,r)}$ for some $M_n^{(s,r)} > 0$. Consider the expression (C.16). Let

$$t_{1,k} := \frac{\left(z_k + \frac{\bar{\alpha}^2}{z_k}\right) \sinh\left(2\bar{\gamma} z_k\right) + 2\bar{\alpha} \cosh\left(2\bar{\gamma} z_k\right)}{\left(z_k + \frac{\bar{\alpha}^2}{z_k}\right) \sinh\left(z_k\right) + 2\bar{\alpha} \cosh\left(z_k\right)}.$$

Note that $\sinh$ and $\cosh$ are isotone functions. Then, since by hypothesis $2\bar{\gamma} < 1$, we have $|t_{1,k}| \leq 1$ for all $k \in \mathbb{N}$. Similarly, letting

$$t_{3,k} := \frac{\left(-z_k + \frac{\bar{\alpha}^2}{z_k}\right) \sinh\left((1 - 2\bar{\gamma}) z_k\right)}{\left(z_k + \frac{\bar{\alpha}^2}{z_k}\right) \sinh\left(z_k\right) + 2\bar{\alpha} \cosh\left(z_k\right)},$$

we have that $|t_{3,k}| \leq 1$ for all $k \in \mathbb{N}$.

Now, let

$$\begin{aligned} t_{2,k} :=& \\ & \frac{4 z_k^{11/2} \left[\frac{\bar{\alpha}}{z_k} \tanh(z_k) + 1\right] \left(z_m + \frac{\bar{\alpha}^2}{z_m}\right) \sin\left((1 - 2\bar{\gamma}) z_m\right)}{z_m^{1/2} \left[\left(z_k + \frac{\bar{\alpha}^2}{z_k}\right) \tanh(z_k) + 2\bar{\alpha}\right] z_m^2 \left(z_m z_k^3 + z_k z_m^3\right)} \\ & \times \frac{\left\{\tanh(z_m) \left[\bar{\alpha}(z_k^2 + z_m^2) \sin(z_k) - z_k(\bar{\alpha}^2 - z_m^2) \cos(z_k)\right] + z_m(\bar{\alpha}^2 + z_k^2) \sin(z_k)\right\}}{\left[\frac{\bar{\alpha}}{z_m} \tanh(z_m) + 1\right] \left[(z_k^2 - \bar{\alpha}^2) \sin(2z_k) + 2z_k(\bar{\alpha}^2 + z_k^2 + \bar{\alpha}) - 2\bar{\alpha} z_k \cos(2z_k)\right]}. \end{aligned}$$

From (C.4) and (C.5) we have

$$\frac{4 z_k^3}{\left[(z_k^2 - \bar{\alpha}^2) \sin(2z_k) + 2z_k(\bar{\alpha}^2 + z_k^2 + \bar{\alpha}) - 2\bar{\alpha} z_k \cos(2z_k)\right]} \leq \frac{1}{\omega H}.$$

From (3.10) we have

$$\sin(z_m) = \frac{2 z_m \bar{\alpha}}{\bar{\alpha}^2 - z_m^2} \cos(z_m).$$

Also, recalling that $z_m \geq z_1$ and that $|\tanh(z)| < 1$,

$$\left|\frac{\bar{\alpha}}{z_k} \tanh(z_k) + 1\right| \leq \frac{\bar{\alpha}}{z_1} + 1, \qquad \left|z_m + \frac{\bar{\alpha}^2}{z_m}\right| \leq z_m \left(1 + \frac{\bar{\alpha}^2}{z_1^2}\right),$$

$$\left|\left(z_k + \frac{\bar{\alpha}^2}{z_k}\right) \tanh(z_k) + 2\bar{\alpha}\right| \geq z_k \left(\tanh(z_1)\right), \qquad \frac{\bar{\alpha}}{z_m} \tanh(z_m) + 1 > 1.$$

We shall obtain a bound for $|t_{2,k}|$ that is independent of k. To that end, we consider several cases. Firstly $z_k \neq \bar{\alpha}$ and $k = 1$; secondly $z_k \neq \bar{\alpha}$ and $k > 1$; and finally, $z_k = \bar{\alpha}$. For $z_k \neq \bar{\alpha}$ it follows that

$$
\begin{aligned}
|t_{2,k}| \leq{}& \frac{\frac{1}{\omega H} z_k^{5/2}\left(\frac{\bar\alpha}{z_1}+1\right) z_m\left(1+\frac{\bar\alpha^2}{z_1^2}\right)}{z_m^{1/2} z_k \tanh(z_1) z_m^2\left(z_m z_k^3 + z_k z_m^3\right)} \\
&\times\left(\bar\alpha(z_k^2+z_m^2)\left|\frac{2z_k\bar\alpha\cos(z_k)}{\bar\alpha^2-z_k^2}\right| + z_k(\bar\alpha^2-z_m^2)|\cos(z_k)|\right. \\
&\left. + z_m(\bar\alpha^2+z_k^2)\frac{2z_k\bar\alpha|\cos(z_k)|}{\bar\alpha^2-z_k^2}\right) \\
\leq{}& \frac{\left(\frac{\bar\alpha}{z_1}+1\right)\left(1+\frac{\bar\alpha^2}{z_1^2}\right)}{\omega H\tanh(z_1)(z_k^2+z_m^2)}\frac{z_k^{1/2}}{z_m^{5/2}} \\
&\times\left(\bar\alpha(z_k^2+z_m^2)\frac{2z_k\bar\alpha|\cos(z_k)|}{z_k^2\left|\frac{\bar\alpha^2}{z_{\min}^2}-1\right|} + z_k(\bar\alpha^2-z_m^2)|\cos(z_k)|\right. \\
&\left. + z_m z_k^2\left(\frac{\bar\alpha^2}{z_k^2}+1\right)\frac{2z_k\bar\alpha|\cos(z_k)|}{z_k^2\left|\frac{\bar\alpha^2}{z_{\min}^2}-1\right|}\right).
\end{aligned}
$$

Let

$$
C(\bar\alpha) = \frac{\left(\frac{\bar\alpha}{z_1}+1\right)\left(1+\frac{\bar\alpha^2}{z_1^2}\right)}{\omega H\left|\frac{\bar\alpha^2}{z_{\min}^2}-1\right|\tanh(z_1)}.
$$

Then, we obtain, using again that $z_k > z_1$,

$$
\begin{aligned}
&|t_{2,k}| \\
&\leq C(\bar\alpha)\left[\frac{2\bar\alpha^2}{z_k^{1/2}}\frac{1}{z_m^{5/2}} + z_k^{3/2}\left(1+\frac{\bar\alpha^2}{z_1^2}\right)\left|\frac{\bar\alpha^2}{z_{\min}^2}-1\right|\frac{1}{z_m^{1/2}(z_k^2+z_m^2)} + \frac{2\bar\alpha z_k^{3/2}\left(\frac{\bar\alpha^2}{z_k^2}+1\right)}{z_m^{3/2}(z_k^2+z_m^2)}\right] \\
&\leq C(\bar\alpha)\left[\frac{2\bar\alpha^2}{z_k^{1/2}}\frac{1}{z_m^{5/2}} + z_k^{3/2}\left(1+\frac{\bar\alpha^2}{z_1^2}\right)\left|\frac{\bar\alpha^2}{z_{\min}^2}-1\right|\frac{1}{z_m^{1/2}(z_k^2+z_m^2)} + \frac{2\bar\alpha\left(\frac{\bar\alpha^2}{z_1^2}+1\right)}{z_m^{3/2}z_1^{1/2}}\right].
\end{aligned}
$$

Thus,

$$
\begin{aligned}
\sum_{m=1}^{\infty}|t_{2,k}| \leq C(\bar\alpha)\Bigg[&\frac{2\bar\alpha^2}{z_k^{1/2}}\left(\sum_{m=1}^{\infty}\frac{1}{z_m^{5/2}}\right) \\
&+ z_k^{3/2}\left(1+\frac{\bar\alpha^2}{z_1^2}\right)\left|\frac{\bar\alpha^2}{z_{\min}^2}-1\right|\left(\sum_{m=1}^{\infty}\frac{1}{z_m^{1/2}(z_k^2+z_m^2)}\right) \\
&+ \frac{2\bar\alpha\left(\frac{\bar\alpha^2}{z_1^2}+1\right)}{z_1^{1/2}}\left(\sum_{m=1}^{\infty}\frac{1}{z_m^{3/2}}\right)\Bigg].
\end{aligned}
\tag{D.2}
$$

Let

$$
S_1 := \sum_{m=1}^{\infty}\frac{1}{z_m^{5/2}}, \qquad S_{2,k} := \sum_{m=1}^{\infty}\frac{1}{z_m^{1/2}(z_k^2+z_m^2)}, \qquad S_3 := \sum_{m=1}^{\infty}\frac{1}{z_m^{3/2}}.
$$

From Lemma F.1 in Appendix F we can see that $S_1 < \infty$ and $S_3 < \infty$. Then, for $k = 1$ we have

$$\begin{aligned}\sum_{m=1}^{\infty} |t_{2,k}| \leq C(\bar{\alpha}) \Bigg[& \frac{2\bar{\alpha}^2}{z_1^{1/2}} \left(\sum_{m=1}^{\infty} \frac{1}{z_m^{5/2}} \right) \\ & + z_1^{3/2} \left(1 + \frac{\bar{\alpha}^2}{z_1^2}\right) \left| \frac{\bar{\alpha}^2}{z_{\min}^2} - 1 \right| \left(\sum_{m=1}^{\infty} \frac{1}{z_m^{5/2}} \right) + \\ & \frac{2\bar{\alpha}\left(\frac{\bar{\alpha}^2}{z_1^2} + 1\right)}{z_1^{1/2}} \left(\sum_{m=1}^{\infty} \frac{1}{z_m^{3/2}} \right) \Bigg] \\ \leq C(\bar{\alpha}) \Bigg[& \frac{2\bar{\alpha}^2}{z_1^{1/2}} S_1 + z_1^{3/2} \left(1 + \frac{\bar{\alpha}^2}{z_1^2}\right) \left| \frac{\bar{\alpha}^2}{z_{\min}^2} - 1 \right| S_1 + \frac{2\bar{\alpha}\left(\frac{\bar{\alpha}^2}{z_1^2} + 1\right)}{z_1^{1/2}} S_3 \Bigg] \\ := C_1 < \infty. \end{aligned}$$

For $k > 1$ and since $(m-1)\pi \leq z_m \leq m\pi$, we have

$$\frac{1}{z_m^{1/2}(z_k^2 + z_m^2)} \leq \frac{1}{[(m-1)\pi]^{1/2} \left[(k-1)^2\pi^2 + (m-1)^2\pi^2\right]} .$$

Then,

$$\begin{aligned} S_{2,k} &= \frac{1}{z_1^{1/2}(z_k^2 + z_1^2)} + \sum_{m=2}^{\infty} \frac{1}{z_m^{1/2}(z_k^2 + z_m^2)} \\ &\leq \frac{1}{z_1^{1/2}(z_k^2 + z_1^2)} + \sum_{m=2}^{\infty} \frac{1}{\pi^{5/2}} \frac{1}{(m-1)^{1/2}\left((k-1)^2 + (m-1)^2\right)} \\ &= \frac{1}{z_1^{1/2}(z_k^2 + z_1^2)} + \frac{1}{\pi^{5/2}} \sum_{j=1}^{\infty} \frac{1}{j^{1/2}\left(\tilde{k}^2 + j^2\right)}, \end{aligned}$$

with $\tilde{k} = k - 1$. Note that

$$\sum_{j=1}^{\infty} \frac{1}{j^{1/2}\left(\tilde{k}^2 + j^2\right)} \leq \int_1^{\infty} \frac{1}{x^{1/2}\left(\tilde{k}^2 + x^2\right)} dx .$$

We bound this integral after a change of variable. Let $u = \frac{\sqrt{x}}{\sqrt{\tilde{k}}}$, so that $dx = 2\tilde{k}^{1/2}\sqrt{x}du$, and $x^2 = \tilde{k}^2 u^4$, thus, using that $u^4 \geq u^2$ for $u \geq 1/\sqrt{\tilde{k}^2}$, we have

$$\begin{aligned} \int_1^{\infty} \frac{1}{x^{1/2}\left(\tilde{k}^2 + x^2\right)} dx &= \frac{2}{\tilde{k}^{3/2}} \int_{1/\sqrt{\tilde{k}^2}}^{\infty} \frac{1}{1+u^4} du \leq \frac{2}{\tilde{k}^{3/2}} \int_0^{\infty} \frac{1}{1+u^2} du \\ &= \frac{2}{\tilde{k}^{3/2}} \lim_{u\to\infty} \arctan(u) = \frac{2}{\tilde{k}^{3/2}} \left(\frac{\pi}{2}\right) = \frac{\pi}{\tilde{k}^{3/2}}. \end{aligned}$$

Before we continue, note that for $k \in \mathbb{N} \setminus \{1\}$ we have

$$\frac{z_k^{3/2}}{\tilde{k}^{3/2}} < \frac{(k\pi)^{3/2}}{(k-1)^{3/2}} = \left(\frac{\pi}{1 - \frac{1}{k}}\right)^{3/2} \leq \left(\frac{\pi}{1 - \frac{1}{2}}\right)^{3/2} = (2\pi)^{3/2} .$$

Then, for $k > 1$, from (D.2), we have

$$\begin{aligned}\sum_{m=1}^{\infty} |t_{2,k}| &\le C(\bar{\alpha}) \left[\frac{2\bar{\alpha}^2}{z_1^{1/2}} S_1 + z_k^{3/2} \left(1 + \frac{\bar{\alpha}^2}{z_1^2}\right) \left| \frac{\bar{\alpha}^2}{z_{\min}^2} - 1 \right| \frac{\pi}{\tilde{k}^{3/2}} + \frac{2\bar{\alpha}\left(\frac{\bar{\alpha}^2}{z_1^2}+1\right)}{z_1^{1/2}} S_3 \right] \\ &\le C(\bar{\alpha}) \left[\frac{2\bar{\alpha}^2}{z_1^{1/2}} S_1 + \left(1 + \frac{\bar{\alpha}^2}{z_1^2}\right) \left| \frac{\bar{\alpha}^2}{z_{\min}^2} - 1 \right| \pi (2\pi)^{3/2} + \frac{2\bar{\alpha}\left(\frac{\bar{\alpha}^2}{z_1^2}+1\right)}{z_1^{1/2}} S_3 \right] \\ &:= C_3 < \infty.\end{aligned}$$

Now, for $z_k = \bar{\alpha}$, we have $\bar{\alpha} = (2j-1)\pi/2$ for some $j \in \mathbb{N}$. Consequently, for $z_k = \bar{\alpha}$ we have $\sin(z_k) = \pm 1$, $\cos(z_k) = 0$, $\sin(2z_k) = 0$, and $\cos(2z_k) = \pm 1$. Then, for $z_k = \bar{\alpha}$ we have

$$\begin{aligned}|t_{2,k}| &\le \frac{z_m \left(4\sqrt{z_k}\left(\frac{\bar{\alpha}}{z_1}+1\right)\left(\frac{\bar{\alpha}^2}{z_1^2}+1\right)\right)\left(\bar{\alpha}\left(z_k^2+z_m^2\right)\tanh(z_m) + z_m\left(\bar{\alpha}^2+z_k^2\right)\right)}{\left(z_k\sqrt{z_m}z_m^2\left(z_m z_k^2 + z_k z_m^2\right)\right)\left(\tanh(z_1)\left(2z_k^3+z_k^2+2\bar{\alpha}^2 z_k\right)\right)} \\ &\le \frac{4\bar{\alpha}^{3/2}\left(\frac{\bar{\alpha}}{z_1}+1\right)\left(\frac{\bar{\alpha}^2}{z_1^2}+1\right)}{\tanh(z_1)(1+4\bar{\alpha})} \frac{1}{z_m^{3/2}\left(\bar{\alpha}^2+z_m^2\right)} \left[\bar{\alpha}\left(\frac{\bar{\alpha}^2}{z_1^2}+1\right) z_m^2 + 2\bar{\alpha}^2 z_m\right] \\ &\le \frac{4\bar{\alpha}^{3/2}\left(\frac{\bar{\alpha}}{z_1}+1\right)\left(\frac{\bar{\alpha}^2}{z_1^2}+1\right)}{\tanh(z_1)(1+4\bar{\alpha})} \left[\bar{\alpha}\left(\frac{\bar{\alpha}^2}{z_1^2}+1\right)\frac{1}{z_m^{3/2}} + 2\bar{\alpha}^2 \frac{1}{z_m^{5/2}}\right].\end{aligned}$$

Then,

$$\begin{aligned}\sum_{m=1}^{\infty} |t_{2,k}| &\le \frac{4\alpha^{3/2}\left(\frac{\alpha}{z_1}+1\right)\left(\frac{\alpha^2}{z_1^2}+1\right)}{\tanh(z_1)(1+4\alpha)} \left[\alpha\left(\frac{\alpha^2}{z_1^2}+1\right)\left(\sum_{m=1}^{\infty}\frac{1}{z_m^{3/2}}\right) + 2\alpha^2\left(\sum_{m=1}^{\infty}\frac{1}{z_m^{5/2}}\right)\right] \\ &= \frac{4\alpha^{3/2}\left(\frac{\alpha}{z_1}+1\right)\left(\frac{\alpha^2}{z_1^2}+1\right)}{\tanh(z_1)(1+4\alpha)} \left[\alpha\left(\frac{\alpha^2}{z_1^2}+1\right) S_3 + 2\alpha^2 S_1\right] := C_4 \cdot\end{aligned}$$

Let $C_5 = \max\{C_1, C_3, C_4\}$. Note that C_5 is independent of k. Then, it follows that

$$\sum_{m=1}^{\infty} |t_{2,k}| \le C_5, \qquad \text{for all } k \in \mathbb{N}.$$

Similarly, letting

$$\begin{aligned}t_{4,k} := &\frac{4z_k^{11/2}\left[\frac{\bar{\alpha}}{z_k}\tanh(z_k)+1\right]\left(z_m + \frac{\bar{\alpha}^2}{z_m}\right)\sin\left((1-2\bar{\gamma})z_m\right)}{z_m^{1/2}\left[\left(z_k+\frac{\bar{\alpha}^2}{z_k}\right)\tanh(z_k)+2\bar{\alpha}\right] z_m^2\left(z_m z_k^3 + z_k z_m^3\right)} \\ &\times \frac{\left\{\tanh(z_m) z_k(\bar{\alpha}^2+z_m^2) - z_m\left[-2\bar{\alpha}z_k + \frac{(\bar{\alpha}^2-z_k^2)\sin(z_k)+2\bar{\alpha}z_k\cos(z_k)}{\cosh(z_m)}\right]\right\}}{\left[\frac{\bar{\alpha}}{z_m}\tanh(z_m)+1\right]\left[(z_k^2) - \bar{\alpha}^2\sin(2z_k) + 2z_k(\bar{\alpha}^2+z_k^2+\bar{\alpha}) - 2\bar{\alpha}z_k\cos(2z_k)\right]}\end{aligned}$$

and using the similar procedure as for $t_{2,k}$, we can see that there exists a constant $C_6 > 0$ such that

$$\sum_{m=1}^{\infty} |t_{4,k}| \le C_6, \qquad \text{for all } k \in \mathbb{N}.$$

Using the results from above and the induction hypothesis, we have that

$$\begin{aligned}|B^{(s,r)}_{n+1,k,1}| &\le |t_{1,k}||B^{(s,r-1)}_{n,k,1}| + \sum_{m=1}^{\infty} |t_{2,k}||B^{(s,r-1)}_{n,m,2}| + |t_{3,k}||B^{(s,r-1)}_{n,k,3}| + \sum_{m=1}^{\infty} |t_{4,k}||B^{(s,r-1)}_{n,m,4}| \\ &\le (1 + C_5 + 1 + C_6) M^{(s,r-1)}_n.\end{aligned}$$

Therefore, with $M^{(s,r)}_{n+1} := (2 + C_5 + C_6) M^{(s,r-1)}_n$, we have that $|B^{(s,r))}_{n+1,k,1}| \le M^{(s,r)}_{n+1}$, for all $k \in \mathbb{N}$. $\square$

Appendix E. Proof of Theorem 4.1.

Proof of Theorem 4.1. Given the initial approximation of the solution u_0, we consider the initial error $\eta_0 = u_0 - u_*$. After the first iteration, all local errors $\eta^{(s,r)}_1$ can be represented in terms of the four parts given by the series (3.14)–(3.17), (3.22)–(3.29). Collecting all the coefficients of these series we have the infinite vector $\mathbf{B}_1$. By Theorem 3.2, the entries of $\mathbf{B}_1$ are bounded; see (3.18). Let us denote by $n_{k_{\max}}$ the order of $\hat{T}_{k_{\max}}$. Let us write the truncated vector $\mathbf{B}^{k_{\max}}_1$ in terms of the eigenvector basis, i.e., $\mathbf{B}^{k_{\max}}_1 = \sum_{j=1}^{n_{k_{\max}}} c_j v^{k_{\max}}_j$. Since the vector $\mathbf{B}^{k_{\max}}_1$ has all its entries bounded, the coefficients in another basis must also be bounded. Let P be such that $c_j \le P$ for all j and for all values of $k_{\max}$. In this proof, to simplify the notation, we will omit the superscript $k_{\max}$ from $v^{k_{\max}}_j$ and $\lambda^{k_{\max}}_j$.

Let $n > n_\epsilon$. Then, we have for a fixed value of $k_{\max}$,

$$\begin{aligned}\|\hat{T}^n_{k_{\max}} \mathbf{B}^{k_{\max}}_1\|_\infty &= \left\| \sum_{j=1}^{n_{k_{\max}}} c_j \lambda^n_j v_j \right\|_\infty = \left\| \sum_{j=1}^{n_{k_{\max}}} \lambda^{n-n_\epsilon}_j (c_j v_j) \lambda^{n_\epsilon}_j \right\|_\infty \\ &\le \sum_{j=1}^{n_{k_{\max}}} |\lambda_j|^{n-n_\epsilon} \|c_j v_j\|_\infty |\lambda^{n_\epsilon}_j| \le \sum_{j=1}^{n_{k_{\max}}} |\lambda_j|^{n-n_\epsilon} \frac{P}{j^{1+\epsilon}} \\ &\le P\rho^{n-n_\epsilon} \sum_{j=1}^{n_{k_{\max}}} \frac{1}{j^{1+\epsilon}} \le P\rho^{n-n_\epsilon} \sum_{j=1}^{\infty} \frac{1}{j^{1+\epsilon}} \le PS\rho^{n-n_\epsilon},\end{aligned}$$

where we have used $S = \sum_{j=1}^{\infty} \frac{1}{j^{1+\epsilon}}$. Thus, we have that $\|\hat{T}^n_{k_{\max}} \mathbf{B}^{k_{\max}}_1\|_\infty \le PS\rho^{n-n_\epsilon}$ for all $k_{\max} \in \mathbb{N}$. Then, it follows that

$$\|\mathbf{B}_{n+1}\|_\infty = \|\hat{T}^n \mathbf{B}_1\|_\infty \le PS\rho^{n-n_\epsilon}. \tag{E.1}$$

Next we bound the local errors. From Lemma G.1 in Appendix G we know that there exists a positive number M such that for all $(x_\ell, y_\ell) \in [0, H]^2$ we have

$$\left|\frac{\phi_m \psi_m}{\psi_m(H)}\right| \le M, \qquad \left|\frac{\phi^{(b)}_m \psi_m}{\psi_m(H)}\right| \le M, \qquad \left|\frac{\phi_m \psi^{(b)}_m}{\cosh(\tilde{z}_m)}\right| \le M, \qquad \left|\frac{\phi^{(b)}_m \psi^{(b)}_m}{\cosh(\tilde{z}_m)}\right| \le M,$$

and

$$\left|(1 + \bar{\alpha}/\tilde{z}_m) \frac{\phi^{(b)}_m \psi^{(b)}_m}{\cosh(\tilde{z}_m)}\right| \le M.$$

Then, from equations (3.14)–(3.17), (3.22)–(3.29), using these bounds as well as (E.1), we can see that the ith part of the local error corresponding to subdomain (s, r) is bounded as

$$|\eta^{(s,r)}_{i,n+1}(x_\ell, y_\ell)| \le \|\mathbf{B}_n\|_\infty M S_2 \le PSMS_2\rho^{n-n_\epsilon},$$

where we used $S_2 = \max\{\sum_{m=1}^{\infty} \frac{1}{z_m^2}, \sum_{m=1}^{\infty} \frac{1}{\tilde{z}_m^2}\}$ and $S_2 < \infty$ as shown in Lemma F.1 in Appendix F. Then, we have the following bound for the local error in the subdomain (s, r):

$$|\eta_{n+1}^{(s,r)}(x_\ell, y_\ell)| = \left| \sum_{i=1}^{4} \eta_{i,n+1}^{(s,r)}(x_\ell, y_\ell) \right| \leq 4PSMS_2\rho^{n-n_\epsilon}.$$

Thus, since the last bound is independent of s, r, x_ℓ, y_ℓ, all the local errors at iteration n are uniformly bounded in $[0, H]^2$ by $4PSMS_2\rho^{n-n_\epsilon}$. Then, since $\rho < 1$, we have that $\eta_{n+1}^{(s,r)}(x_\ell, y_\ell)$ tends to zero uniformly in $(x_\ell, y_\ell) \in [0, H]^2$, $s \in \{1, \ldots, p\}$, and $r \in \{1, \ldots, q\}$ as n tends to infinity. Consequently, given that all local errors converge to zero, the (synchronous) optimized Schwarz iteration converges to the solution of (2.1). $\square$

Appendix F. The series with roots of the transcendental equation is convergent.

LEMMA F.1. *Let z_m be the solutions of (3.10). Then, $\sum_{m=1}^{\infty} \frac{1}{z_m^2} < \infty$.*

The solutions of (3.10) are the zeros of the function $\Phi : \mathbb{R} \to \mathbb{R}$, $\Phi(z) = \tan(z) - \frac{2z\bar{\alpha}}{\bar{\alpha}^2 - z^2}$. Thus, z_m is a positive zero of Φ for all $m \in \mathbb{N}$. Plotting the graph of Φ we can see that $z_m > (m-1)\pi$ for all $m \in \mathbb{N}$ (see Figure F.1). Then we have

$$\sum_{m=1}^{\infty} \frac{1}{z_m^2} = \frac{1}{z_1^2} + \sum_{m=2}^{\infty} \frac{1}{z_m^2} \leq \frac{1}{z_1^2} + \sum_{m=2}^{\infty} \frac{1}{((m-1)\pi)^2} = \frac{1}{z_1^2} + \frac{1}{\pi^2} \sum_{j=1}^{\infty} \frac{1}{j^2}.$$

Note that $\sum_{j=1}^{\infty} \frac{1}{j^a} < \infty$ for any $a > 1$. Then, $\sum_{j=1}^{\infty} \frac{1}{j^2} < \infty$. Consequently, since $z_1 > 0$ and $\sum_{j=1}^{\infty} \frac{1}{j^2} < \infty$, we have $\sum_{m=1}^{\infty} \frac{1}{z_m^2} < \infty$. $\square$

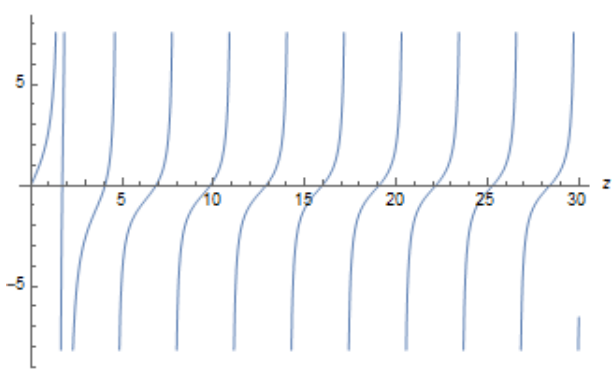

FIG. F.1. *Graph of Φ for $\bar{\alpha} = 2$. Note that z_m is the mth positive zero of Φ.*

Appendix G. Bounds for functions for the generalized Fourier series.

LEMMA G.1. *There exists a positive constant $M > 0$, independent of m, such that*

$$\left| \frac{\phi_m \psi_m}{\psi_m(H)} \right| \leq M, \qquad \left| \frac{\phi_m^{(b)} \psi_m}{\psi_m(H)} \right| \leq M, \qquad \left| \frac{\phi_m \psi_m^{(b)}}{\cosh(\tilde{z}_m)} \right| \leq M, \qquad \left| \frac{\phi_m^{(b)} \psi_m^{(b)}}{\cosh(\tilde{z}_m)} \right| \leq M,$$

and

$$\left| (1 + \bar{\alpha}/\tilde{z}_m) \frac{\phi_m^{(b)} \psi_m^{(b)}}{\cosh(\tilde{z}_m)} \right| \leq M,$$

where ϕ_m, ψ_m,$\phi_m^{(b)}$, $\psi_m^{(b)}$ *are defined in equations* (3.8), (3.9), (3.20), *and* (3.19), *respectively.*

Proof. We can easily bound the following:

$$\frac{\psi_m}{\psi_m(H)} = \frac{\frac{\bar{\alpha}}{z_m}\sinh\left(\frac{z_m x}{H}\right) + \cosh\left(\frac{z_m x}{H}\right)}{\frac{\bar{\alpha}}{z_m}\sinh\left(z_m\right) + \cosh\left(z_m\right)} \leq \frac{\frac{\bar{\alpha}}{z_m}\sinh\left(\frac{z_m x}{H}\right) + \cosh\left(\frac{z_m x}{H}\right)}{\cosh(z_m)} .$$

Since $\sinh$ and $\cosh$ are isotone functions,

$$\sinh\left(\frac{z_m x}{H}\right) \leq \sinh\left(\frac{z_m H}{H}\right) = \sinh(z_m), \quad \cosh\left(\frac{z_m x}{H}\right) \leq \cosh\left(\frac{z_m H}{H}\right) = \cosh(z_m)$$

and since $\sinh(x) \leq \cosh(x)$ for all $x \in \mathbb{R}$, we have

$$\frac{\sinh\left(\frac{z_m x}{H}\right)}{\cosh(z_m)} \leq 1, \qquad \frac{\cosh\left(\frac{z_m x}{H}\right)}{\cosh(z_m)} \leq 1.$$

Then, recalling that $z_m \geq z_1$,

$$\frac{\psi_m}{\psi_m(H)} \leq \frac{\bar{\alpha}}{z_m} + 1 \leq \frac{\bar{\alpha}}{z_1} + 1.$$

Similarly, we have

$$\begin{aligned}
\frac{\psi_m^{(b)}}{\cosh(\tilde{z}_m)} &= \frac{\sinh\left(\frac{\tilde{z}_m x}{H}\right)}{\cosh(\tilde{z}_m)}, \\
\phi_m(x) &= \frac{\bar{\alpha}}{z_m}\sin\left(\frac{z_m x}{H}\right) + \cos\left(\frac{z_m x}{H}\right) \leq \frac{\bar{\alpha}}{z_1} + 1, \qquad \text{and} \\
\phi_m^{(b)}(x) &= \sin\left(\frac{\tilde{z}_m x}{H}\right) \leq 1.
\end{aligned}$$

Thus, we can write the following bounds:

$$|\phi_m(x)| \leq \frac{\bar{\alpha}}{z_1} + 1, \quad \left|\phi_m^{(b)}(x)\right| \leq \frac{\bar{\alpha}}{z_1} + 1, \quad \left|\frac{\psi_m(x)}{\psi_m(H)}\right| \leq \frac{\bar{\alpha}}{z_1} + 1, \quad \left|\frac{\psi_m^{(b)}(x)}{\cosh(\tilde{z}_m)}\right| \leq \frac{\bar{\alpha}}{z_1} + 1.$$

Then, letting $M := \left(\frac{\bar{\alpha}}{z_1} + 1\right)^2 \left(\frac{\bar{\alpha}}{\tilde{z}_1} + 1\right)$ we have

$$\left|\frac{\phi_m \psi_m}{\psi_m(H)}\right| \leq M, \quad \left|\frac{\phi_m^{(b)} \psi}{\psi_m(H)}\right| \leq M, \quad \left|\frac{\phi_m \psi_m^{(b)}}{\cosh(\tilde{z}_m)}\right| \leq M, \quad \left|\frac{\phi_m^{(b)} \psi_m^{(b)}}{\cosh(\tilde{z}_m)}\right| \leq M, \qquad \text{and}$$

$$\left|(1 + \bar{\alpha}/\tilde{z}_m)\frac{\phi_m^{(b)} \psi_m^{(b)}}{\cosh(\tilde{z}_m)}\right| \leq M . \qquad \square$$

REFERENCES

[1] ARGONNE NATIONAL LABORATORY, *MPI: The Message Passing Interface*, Mathematics and Computer Science Division, Argonne National Laboratory, Lemont, 1993.

[2] J. BAHI, *Algorithmes parallèles asynchrones pour des systèmes singuliers*, C. R. Acad. Sci. Paris Sér. I Math., 326 (1998), pp. 1421–1425.

[3] J. M. BAHI, S. CONTASSOT-VIVIER, AND R. COUTURIER, *Parallel Iterative Algorithms*, CRC Press, Boca Raton, 2007.

[4] B. BARÁN, E. KASZKUREWICZ, AND A. BHAYA, *Parallel asynchronous team algorithms: convergence and performance analysis*, IEEE Trans. Parallel Distrib. Systems, 7 (1996), pp. 677–688.

[5] G. M. BAUDET, *Asynchronous iterative methods for multiprocessors*, J. Assoc. Comput. Mach., 25 (1978), pp. 226–244.

[6] D. P. BERTSEKAS, *Distributed asynchronous computation of fixed points*, Math. Programming, 27 (1983), pp. 107–120.

[7] D. P. BERTSEKAS AND J. N. TSITSIKLIS, *Parallel and Distributed Computation: Numerical Methods*, Prentice-Hall, Englewood Cliffs, 1989.

[8] R. BRU, V. MIGALLÓN, AND J. PENADÉS, *Chaotic methods for the parallel solution of linear systems*, Computing Systems Eng., 6 (1995), pp. 385–390.

[9] D. CHAZAN AND W. MIRANKER, *Chaotic relaxation*, Linear Algebra Appl., 2 (1969), pp. 199–222.

[10] G. CIARAMELLA AND M. J. GANDER, *Analysis of the parallel Schwarz method for growing chains of fixed-sized subdomains: Part I*, SIAM J. Numer. Anal., 55 (2017), pp. 1330–1356.

[11] V. DOLEAN, P. JOLIVET, AND F. NATAF, *An Introduction to Domain Decomposition Methods*, SIAM, Philadelphia, 2015.

[12] D. EL BAZ, D. GAZEN, J.-C. MIELLOU, AND P. SPITERI, *Mise en œuvre de méthodes itératives asynchrones avec communication flexible, application à la résolution d'une classe de problèmes d'optimisation*, Calculateurs Parallèles, 8 (1996), pp. 393–410.

[13] D. EL BAZ, P. SPITERI, J.-C. MIELLOU, AND D. GAZEN, *Asynchronous iterative algorithms with flexible communication for nonlinear network flow problems*, J. Parallel Distributed Comput., 38 (1996), pp. 1–15.

[14] M. EL HADDAD, J. C. GARAY, F. MAGOULÈS, AND D. B. SZYLD, *Synchronous and asynchronous optimized Schwarz methods for one-way subdivision of bounded domains*, Numer. Linear Algebra Appl., 27 (2020), Art. e2279, 30 pages.

[15] M. N. EL TARAZI, *Some convergence results for asynchronous algorithms*, Numer. Math., 39 (1982), pp. 325–340.

[16] L. ELSNER, I. KOLTRACHT, AND M. NEUMANN, *Convergence of sequential and asynchronous nonlinear paracontractions*, Numer. Math., 62 (1992), pp. 305–319.

[17] A. FROMMER, *On asynchronous iterations in partially ordered spaces*, Numer. Funct. Anal. Optim., 12 (1991), pp. 315–325.

[18] A. FROMMER AND D. B. SZYLD, *Asynchronous two-stage iterative methods*, Numer. Math., 69 (1994), pp. 141–153.

[19] ———, *On asynchronous iterations*, J. Comput. Appl. Math., 123 (2000), pp. 201–216.

[20] M. J. GANDER, *Optimized Schwarz methods*, SIAM J. Numer. Anal., 44 (2006), pp. 699–731.

[21] J. C. GARAY, F. MAGOULÈS, AND D. B. SZYLD, *Convergence of asynchronous optimized Schwarz methods in the plane*, in Domain Decomposition Methods in Science and Engineering XXIV, P. E. Bjørstad, S. C. Brenner, L. Halpern, H. H. Kim, R. Kornhuber, T. Rahman, and O. B. Widlund, eds., vol. 125 of Lect. Notes Comput. Sci. Eng., Springer, Cham, 2018, pp. 333–341.

[22] ———, *Optimized Schwarz method for Poisson's equation in rectangular domains*, in Domain Decomposition Methods in Science and Engineering XXIV, P. E. Bjørstad, S. C. Brenner, L. Halpern, H. H. Kim, R. Kornhuber, T. Rahman, and O. B. Widlund, eds., vol. 125 of Lect. Notes Comput. Sci. Eng., Springer, Cham, 2018, pp. 533–541.

[23] C. GLUSA, E. G. BOMAN, E. CHOW, S. RAJAMANICKAM, AND D. B. SZYLD, *Scalable asynchronous domain decomposition solvers*, SIAM J. Sci. Comput., 42 (2020), pp. C384–C409.

[24] R. HABERMAN, *Applied Partial Differential Equations with Fourier Series and Boundary Value problems*, 4th ed., Prentice Hall, Englewood Cliffs, 2003.

[25] G. KARYPIS AND V. KUMAR, *MeTis: Unstructured Graph Partitioning and Sparse Matrix Ordering System, Version 4.0*, Manual MN55455, Department of Computer Science, University of Minnesota, Minneapolis, 2009.

[26] M. KREĬN AND M. RUTMAN, *Linear operators leaving invariant a cone in a Banach space*, Amer. Math. Soc. Translation 1950, 26 (1950), 128 pages.

[27] B. LUBACHEVSKY AND D. MITRA, *A chaotic asynchronous algorithm for computing the fixed point of a nonnegative matrix of unit spectral radius*, J. Assoc. Comput. Mach., 33 (1986), pp. 130–150.

[28] F. MAGOULÈS AND A.-K. CHEIK AHAMED, *Alinea: an advanced linear algebra library for massively parallel computations on graphics processing units*, Int. J. High Performance Comput. Appl., 29 (2015), pp. 284–310.

[29] F. MAGOULÈS, A.-K. CHEIK AHAMED, AND R. PUTANOWICZ, *Optimized Schwarz method without overlap for the gravitational potential equation on cluster of graphics processing unit*, Int. J. Comput. Math., 93 (2016), pp. 955–980.

[30] F. MAGOULÈS AND G. GBIKPI-BENISSAN, *JACK: An asynchronous communication kernel for massively parallel computations.*, J. Supercomputing, 73 (2007), pp. 3468–3487.

[31] ———, *Distributed convergence detection based on global residual error under asynchronous iterations*, IEEE Trans. Parallel Distrib. Systems, 29 (2018), pp. 819–829.

[32] F. MAGOULÈS, P. IVÁNYI, AND B. H. V. TOPPING, *Non-overlapping Schwarz methods with optimized transmission conditions for the Helmholtz equation*, Comput. Methods Appl. Mech. Engrg., 193 (2004), pp. 4797–4818.

[33] F. MAGOULÈS, D. B. SZYLD, AND C. VENET, *Asynchronous optimized Schwarz methods with and without overlap*, Numer. Math., 137 (2017), pp. 199–227.

[34] I. MAREK AND D. B. SZYLD, *Splittings of M-operators: irreducibility and the index of the iteration operator*, Numer. Funct. Anal. Optim., 11 (1990), pp. 529–553.

[35] J.-C. MIELLOU, P. CORTYE-DUMONT, AND M. BOULBRACHÊNE, *Perturbation of fixed-point iterative methods*, Adv. Parallel Comput., 1 (1990), pp. 81–122.

[36] F. ROBERT, *Contraction en norme vectorielle: convergence d'iterations chaotiques pour des equations non linéaires de point fixe à plusiers variables*, Linear Algebra Appl., 13 (1976), pp. 19–35.

[37] P. SPITERI, *Parallel asynchronous algorithms: a survey*, Adv. Eng. Software, 149 (2020), Art. 102896, 34 pages.

[38] D. B. SZYLD, *Different models of parallel asynchronous iterations with overlapping blocks*, Comput. Appl. Math., 17 (1998), pp. 101–115.

[39] A. TOSELLI AND O. B. WIDLUND, *Domain Decomposition Methods—Algorithms and Theory*, Springer, Berlin, 2005.